

PILOT STUDY OF A HIGH CAPACITY DUCTILE
SEISMIC HOLDOWN FOR CROSS LAMINATED TIMBER

by

John Howison Nicholas

A thesis submitted in partial fulfillment
of the requirements for the degree

of

Master of Science

In

Civil Engineering

MONTANA STATE UNIVERSITY
Bozeman, Montana

May 2019

©COPYRIGHT

by

John Howison Nicholas

2019

All Rights Reserved

ACKNOWLEDGEMENTS

I would like to thank my committee chairman, Dr. Damon Fick, who allowed me to complete my thesis at Montana State University. I would also like to thank the other members of my committee, Dr. Richard Schmidt and Dr. Ladean McKittrick, who provided substantial contributions to my academic mentorship as a structural engineer and supplemented a wealth of technical knowledge necessary for my research.

I would like to acknowledge Max Closen and his team at MyTiCon for helping me establish a wood research project to be carried out at Montana State University and providing the fasteners used to complete my research. Additionally, I would like to thank Jim Henjum and his team at Smartlam for providing the CLT specimens used to complete the testing for this project.

I would like to express my gratitude to Theron Thompson and Stahly Engineering & Associates for allowing me the opportunity to obtain my graduate degree and funding my coursework while employing me. Also, I would like to acknowledge support from a Faculty Excellence Grant funded from MSU's Provost office to support the experimental portion of the project.

Finally, I would like to thank my wife, Grace Nicholas, who provided the necessary support to allow me to pursue my graduate degree. Without her support my path through graduate school would not have been feasible.

TABLE OF CONTENTS

1. INTRODUCTION	1
Background.....	1
Motivation.....	2
Ductility Sources in Light-Framed Wood Structures	3
Objectives	4
Organization.....	5
2. LITERATURE REVIEW	6
Fastener Behavior Tests.....	6
Shear Wall Assembly Tests	9
Dissipative Connector Tests	11
Scope and Limitations	15
3. EXPERIMENTAL PROGRAM	18
Materials	18
Self-Drilling Dowel	18
CLT Panels.....	20
Steel Plates	21
Small-Scale Exploratory Tests.....	22
Fastener Bending and Shear Tests	22
Single Knife Plate Tests.....	25
Double Knife Plate Tests	28
Reduced Section Steel Plate Modeling	32
Reduced Section Small-Scale Steel Plate Tests.....	33
CLT Shear Wall Test	36
4. RESULTS & DISCUSSION.....	44
Small Scale Exploratory Tests.....	44
Fastener Bending and Shear Tests	44
Single Knife Plate Tests.....	51
Double Knife Plate Tests	58
Reduced Section Steel Plate Models and Tests	62
CLT Shear Wall Test	69
5. SUMMARY & CONCLUSION	79
6. FUTUTRE WORK	82

LIST OF TABLES

Table	Page
1. Fastener Material Properties	19
2. SDD Bending Test Results	47
3. SDD Shear Test Results	49
4. Single Knife Plate Single Fastener Test Results	53
5. Single Knife Plate Group Fastener Test Results	54
6. Double Knife Plate Single Fastener Test Results	59
7. Double Knife Plate Group Fastener Test Results	60
8. Small Scale Plate Reaction Summary	67

LIST OF FIGURES

Figure	Page
1. Inclined fastener experimental setup (Hossain et al., 2016)	7
2. Inclined fastener load-displacement curves (Hossain et al., 2016).....	8
3. Conventional high strength holdown test specimen (Popovski et al., 2010)	9
4. Conventional holdown load-displacement curves (Popovski et al., 2010).....	10
5. XL-stub holdown connections tests (Latour & Rizzano, 2017)	11
6. Load-displacement response of XL-stub (Latour & Rizzano, 2017).....	13
7. Adhesive knife plate connection setup (Zhang et al., 2018).....	14
8. Adhesive holdown load-displacement response (Zhang et al., 2018)	15
9. Knife plate configurations.....	16
10. Self-drilling dowel	19
11. 5-maxx CLT panel	20
12. 5-alt CLT panel.....	21
13. Fastener bending test setup	23
14. Fastener bending test layout.....	23
15. Fastener shear test setup.....	24
16. Fastener shear test layout	24
17. Single knife plate single fastener test layout.....	26
18. Single knife plate group fastener test layout.....	27
19. Single knife plate test setups.....	28
20. Double knife plate single fastener layout.....	30

LIST OF FIGURES CONTINUED

Figure	Page
21. Double knife plate group fastener layout.....	31
22. Double knife plate tests setups.....	32
23. Small-scale reduced section plate layout	35
24. Small scale reduced section test assembly.....	36
25. Full-scale reduced section plate layout.....	38
26. CLT shear wall assembly layout.....	39
27. Full-scale knife plate slots	40
28. Full-scale holdown assembly.....	41
29. CLT shear wall assembly.....	43
30. NDS connection yield modes (American Wood Council, 2017).....	45
31. Load-deformation diagram for bending test (ASTM International, 2008).....	46
32. SDD bending test load-displacement.....	47
33. SDD bending failure	48
34. SDD shear test load-displacement	50
35. SDD shear failure.....	51
36. Coefficients of variation for clear wood mechanical properties (Forest Products Laboratory, 2010)	52
37. Single knife plate single fastener load-displacement.....	54
38. Single knife plate group fastener load-displacement.....	55
39. Single knife plate single fastener failure.....	56

LIST OF FIGURES CONTINUED

Figure	Page
40. Single knife plate group fastener failure.....	57
41. Double knife plate single fastener load-displacement	59
42. Double knife plate group fastener load-displacement	60
43. Single vs. double knife plate group fastener tests.....	61
44. ANSYS small-scale plate element deflection plot.....	63
45. ANSYS small-scale Von Mises element stress plot	64
46. Small-scale reduced section deformed plate.....	66
47. Small scale loading tab displacement	68
48. Small-scale reduced section load-displacement curve.....	69
49. ANSYS full-scale plate element deflection plot.....	70
50. ANSYS full-scale plate Von Mises element stress plot.....	71
51. CLT shear wall cycle 1a lateral load-displacement plot.....	73
52. CLT holdown vertical load-displacement plot	74
53. Tested full-scale reduced section knife plate	75
54. Tested shear wall fastener.....	76
55. Tested CLT panel fastener holes.....	76
56. HSS wall buckling failure.....	77

ABSTRACT

New manufactured wood products referred to as mass timber have allowed for greater seismic load capacities than ever before for designing wood structures. The increased capacities could allow for taller wood structures; however, traditional wood connections do not meet the seismic performance needs for new manufactured wood products such as cross laminated timber (CLT). New connection methods must be investigated to allow for the growth of the CLT industry in mid- and high-rise structures.

The objective of this research is to develop a wood connection to resist larger uplift forces experienced in CLT structures and provide energy dissipation in seismic events. The connection development was performed through fastener testing using self-drilling dowel fasteners for concealed connections with steel knife plates installed in a wood member. Finite element modeling and testing of reduced section steel plate to provide a ductile response to cyclic loading was performed to determine the feasibility of this connections style. The results of the investigation indicate that reduced section steel plates that limit the connection failure to a desired location in the steel plate could greatly increase the seismic performance of CLT seismic force resisting systems.

INTRODUCTION

Background

Timber has been one of the most common building materials used in the construction industry throughout history. Traditionally, timber is readily available and can be used without advanced manufacturing techniques or equipment. Throughout the 20th century, building materials and manufacturing have rapidly advanced, leading to the engineered wood products industry. Engineered wood products utilize wood mill scraps, small diameter logs, and adhesives to achieve greater element strengths than are achievable through harvesting old-growth large timbers. One of the more recent trends in the engineered wood products industry is cross laminated timber (CLT), where dimensional lumber (1x6 or 2x6) is layered in orthogonal plies and laminated together with adhesives to form larger structural panels. CLT and similar forms of mass timber have created new opportunities for wood products in construction of buildings that are stronger and more durable than traditional light-framed wood structures.

The progressive use of engineered wood products and their increased strength requires development of new connection methods to efficiently utilize element capacities. Plate connections with dowel-type fasteners such as bolts, lag screws, screws, and nails are currently the standard of practice for connecting timber and light-framed wood elements allowing for dowel-type fasteners to join two elements in shear or tension. Currently available proprietary plate connectors, however, were not designed for the increased strength of CLT members and do not take advantage of the rigid panel

behavior. The development of high strength CLT connections provides an opportunity to continue the progression of timber design, thereby enabling wood to compete with alternative building materials in mid-rise and high-rise structures.

Motivation

CLT is rapidly becoming an accessible option for construction of low-rise and mid-rise structures throughout North America. Regions in Europe have developed substantial markets for CLT in residential and commercial construction and have more advanced acceptance in building codes for design of CLT structures. As CLT begins its progression into building codes throughout North America, one challenge the industry faces is providing structural ductility in response to cyclic loading during seismic events. Due to the high stiffness of CLT members, the panels essentially behave as rigid bodies under in-plane loading and provide very little energy dissipation during strong ground motions. The rigid response of CLT panels requires that ductility be achieved through panel connections to avoid brittle failures of the wood panel.

Energy dissipation is a primary objective in the design of structures in seismic regions. The ground accelerations developed during a seismic event can cause the structure to experience rapid cyclic lateral loads. To dissipate the energy within a structure during such an event, the materials of the lateral-force resisting system must be capable of yielding in a ductile manner to avoid brittle and potentially catastrophic failures. The International Building Code (International Code Council, 2012) (IBC) prescribes seismic response modification factors for different building structure types that

are inversely related to the magnitude of lateral seismic forces used to design a building's structural system. The code-prescribed lateral seismic design forces are substantially higher for structures that do not provide a ductile response under cyclic loading. CLT structural systems have lower seismic design forces through their lighter mass compared to steel and concrete structural systems, but do not provide the ductility that is achieved through yielding of steel cross sections and reinforcement. Despite their lighter weight, the lack of ductility in CLT lateral-force-resisting systems results in higher lateral design forces. Higher design forces required for CLT panels currently hinders the economical use of CLT shear walls in many mid-rise and high-rise structures.

Ductility Sources in Light-Framed Wood Structures

The most common connection style used to transfer shear forces in wood structures utilizes single shear connections with metal dowel-type fasteners. This practice offers a ductile response for wood shear connections when loaded in one direction due to flexural yielding of the fastener and crushing of the wood, however, when loaded cyclically, less energy dissipation occurs following each subsequent cycle. The loss of energy dissipation is due to the permanent deformation of the crushed wood, resulting in a pinched hysteresis loop. Traditional wood connection design is controlled by dowel fastener yielding combined with wood crushing and does not utilize yielding of a plate connector, thereby limiting ideal energy dissipation to one cycle. Due to the redundancies in light-framed wood construction and structure height limitations, this method of energy

dissipation has been sufficient. However, CLT design is targeting less redundant mid- and high-rise structural systems.

The primary energy dissipation method for light-frame wood shear walls with wood sheathing is through yielding of multiple sheathing fasteners (Think Wood, 2015). The lateral connection of the diaphragm to the top plate and the holddown at each end of the light-framed shear wall resisting uplift provide relatively little ductility to the lateral-force resisting system due to the limited number of fasteners compared to the shear wall sheathing. Because CLT lateral systems do not have sheathing fastened with many nails, the cyclic ductility required in larger structures must be provided through boundary connections such as panel splices and foundation anchorage connections.

One advantage of the high strength and stiffness of CLT shear walls relative to light-framed walls is their ability to utilize slender panels capable of withstanding increased loading to achieve a more desirable architectural design. The increased lateral loads on slender elements results in larger uplift forces than light-framed wood-sheathed shear walls. Conventional holddowns designed for light-framed wood structures are only able to utilize a small fraction of the strength of CLT members.

Objectives

The overall objective of this research is to develop and characterize the ductile behavior of a high-strength holddown connection for CLT walls while maintaining a practical field installation process. The preliminary investigation utilized small-scale fastener connection tests to identify the bending yield and shear strength of the fasteners

and the load-displacement curve of the fasteners in knife-plate assemblies with CLT specimens. Finite element analysis models were used to identify appropriate connection geometry for the reduced section steel plate to obtain a ductile response for the holdown connection during cyclic loading. The specific objectives include: 1) determining the load-displacement response for the fasteners utilized in this research 2) developing a knife-plate connection with self-tapping screws that provides adequate strength and ductility for CLT shear walls, 3) quantifying the load-displacement response for the developed CLT shear wall system, and 4) identifying suitable building types and geometries where the developed shear wall system is an economical option for resisting seismic loading. The developed holdown will provide the primary source of ductility within the shear wall system and will achieve capacities currently unavailable for conventional proprietary holdowns. The results of the research will provide a high ductility connection that could be used in holdowns, panel splices and other shear connections in mass timber structures.

Organization

Chapter 20 of this thesis provides a literature review of previous research on fastener behavior, CLT shear wall assemblies, and dissipative steel plate connectors. Chapter 3 discusses the experimental program and testing methods used to complete this research. Chapter 4 includes the experimental program and analytical modeling results and a discussion of the findings. A summary and conclusions are presented in Chapter 5 followed by potential future works in Chapter 6.

LITERATURE REVIEW

A substantial amount of testing has been performed recently on CLT connections and CLT shear wall assemblies. CLT connection test are typically controlled by the interaction between the fastener and wood panel. Many fastener tests result in yielding of the fastener and crushing of the wood grain, providing limited strength and ductility under cyclic loading. Publicly available research related to plate connectors designed to yield during strong ground motions for energy dissipation in CLT shear wall systems is limited. A summary of the recent analytical and experimental research related to fastener behavior, CLT shear wall assemblies, and dissipative steel plate connectors is included below and is used to validate the approach for this research.

Fastener Behavior Tests

Hossain, Danzig, and Tannert (2016) performed a study on inclined self-tapping screw assemblies for CLT toe-screwed panel splice connections. Twenty fully-threaded fasteners per shear plane spaced at 90 mm were angled in opposite directions of butt-splice connections and were tested for shear resistance in monotonic and cyclic loading. The load was applied through a uniaxial test assembly using vertical loads to induce shear across the butt-splice connections. This test configuration is shown in Figure 1.

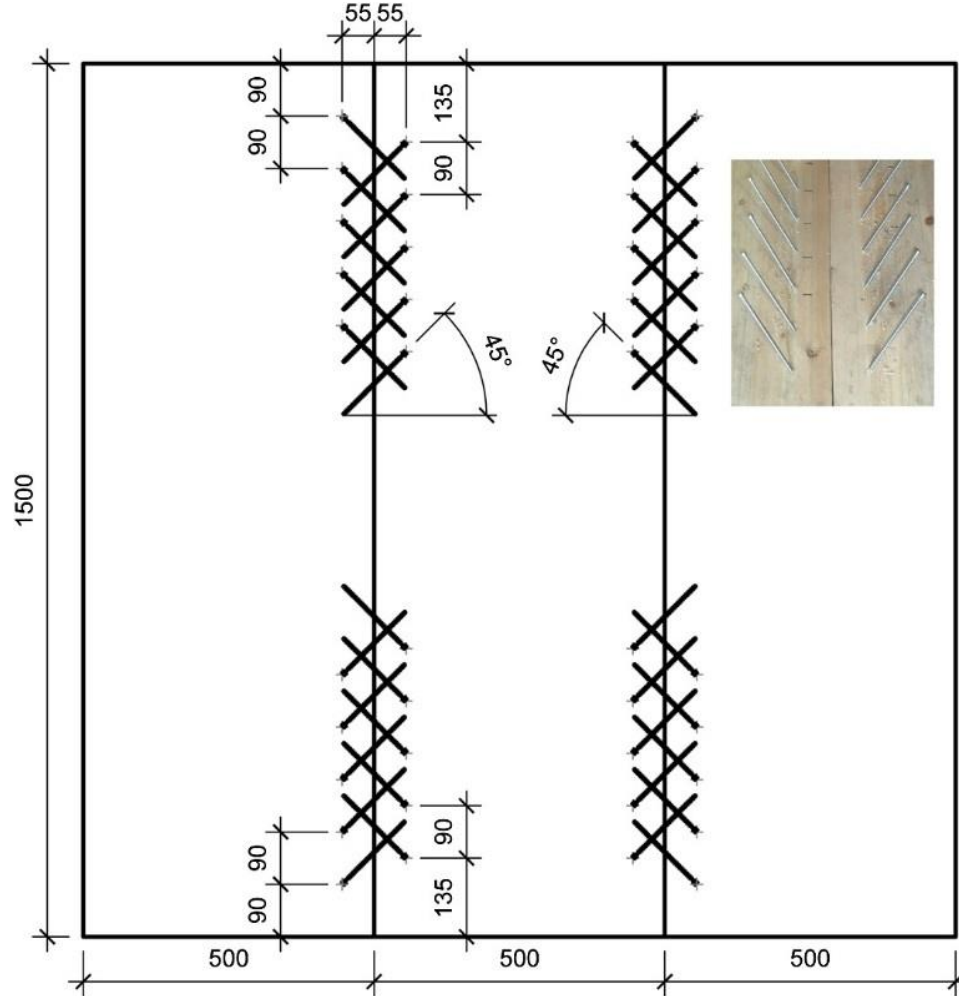


Figure 1 Inclined fastener experimental setup (Hossain et al., 2016)

The findings of this study confirmed that inclined fastener connections perform well under monotonic loading, displaying no rapid loss in applied load during failure. The angled fasteners prohibited panel splitting and exhibited a stiffer connection with increased energy dissipation compared to non-inclined connections. When the same assembly was subjected to cyclic load tests, some of the specimens failed with an abrupt loss of load, limiting the energy dissipation achieved in subsequent cycles. The initial upward actuator stroke caused half of the screws to partially withdrawal from the CLT

panel and limited the fastener's ability to carry compression loading when the actuator reversed. The initial upward stroke carried approximately 20 percent more load than the following downward stroke. Although the connection demonstrated increased ductility relative to non-inclined connections, it still displayed pinched hysteresis loops with substantial capacity losses in later cycles due to initial fastener withdrawal and wood crushing as shown in Figure 2.

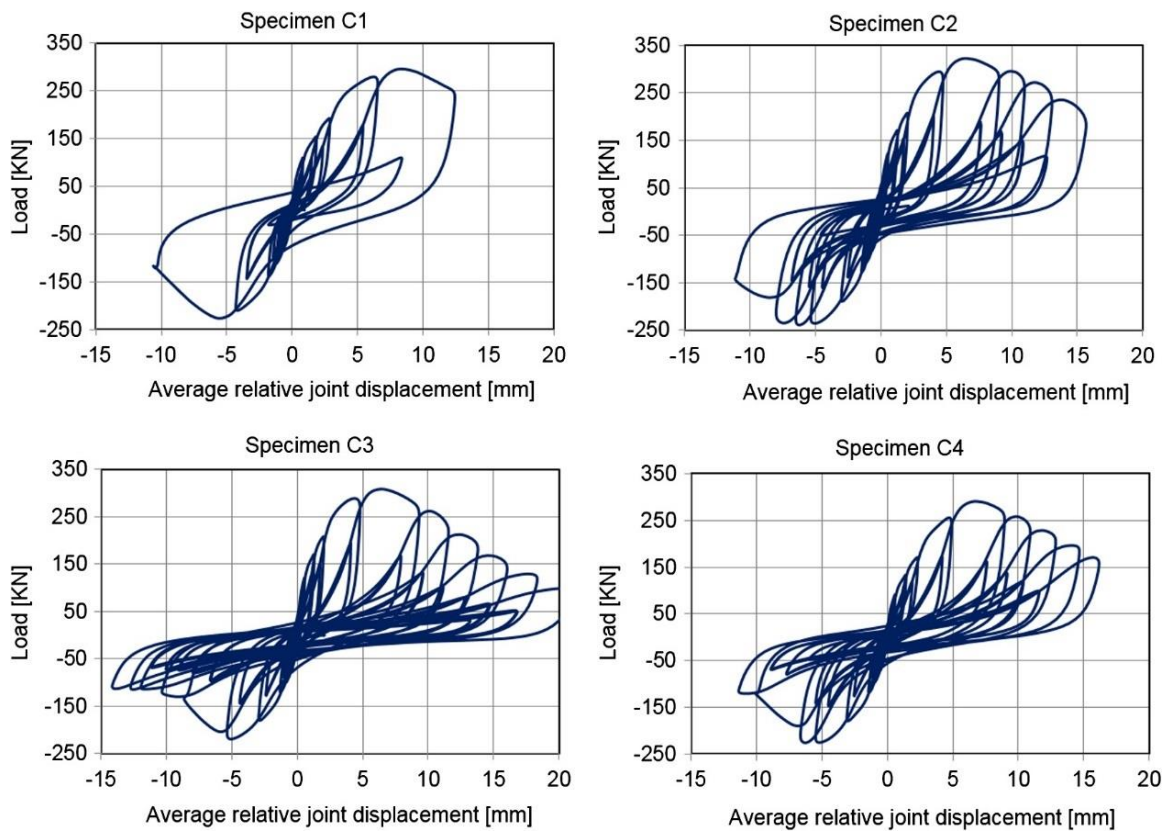


Figure 2 Inclined fastener load-displacement curves (Hossain et al., 2016)

Shear Wall Assembly Tests

The research performed by Popovski, Schneider, and Schweinsteiger (2010) addressed full scale CLT shear wall assemblies using traditional steel plate connectors with a variety of fasteners and geometries. Combinations of light gauge steel angles and heavy gauge rigid steel holdowns were fastened to the CLT panels with nails, screws, and timber rivets. The high capacity steel holdowns were manufactured using 6.4 mm thick steel plate to allow up to 40 timber rivets to be driven into the face of a CLT panel. The timber rivets formed a wood shear plug failure when spaced inadequately, causing the outer plies of the CLT to fracture and delaminate in a brittle failure. A representative test specimen with 20 timber rivets is shown in Figure 3a and the shear plug failure with 40 timber rivets is shown in Figure 3b.



(a)



(b)

Figure 3 Conventional high strength holdown test specimen (Popovski et al., 2010)

In all cases the CLT specimens behaved nearly as rigid bodies providing very little shear deformation. Most of the panel deflection was a result of the panel boundary connections designed to meet fastener yield modes. The resulting hysteresis loops shown in Figure 4 contained pinched curves reflecting the poor cyclic behavior of traditional wood plate connections. The thick red curve represents the monotonic load-displacement response while the thinner blue curves represent the cyclic response. The testing performed in this researched confirmed that CLT panels are very stiff elements and their design is typically controlled by the boundary connections rather than the panel behavior.

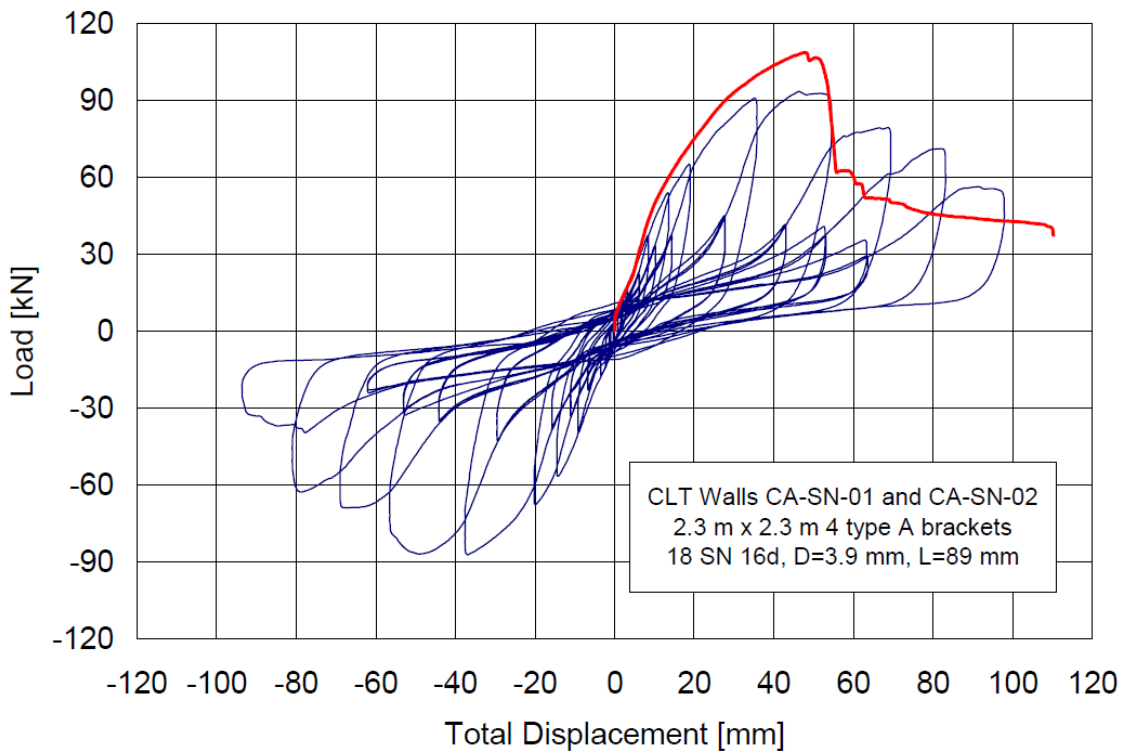


Figure 4 Conventional holdown load-displacement curves (Popovski et al., 2010)

Dissipative Connector Tests

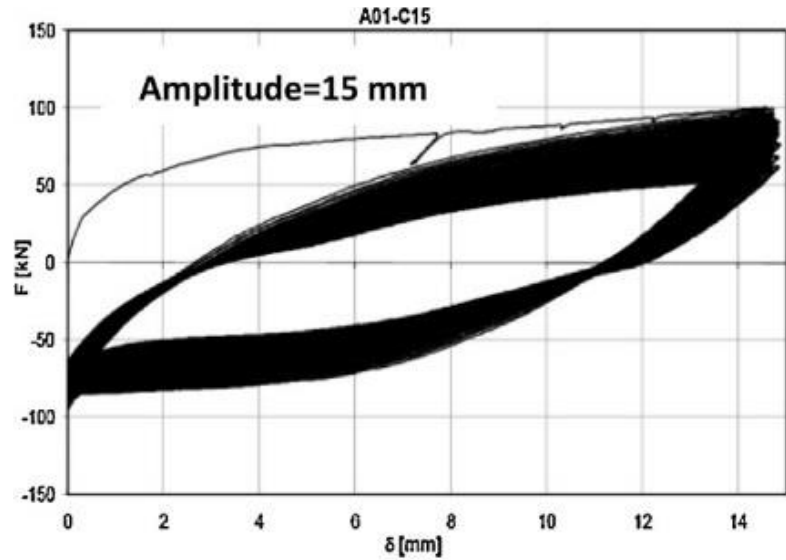
Latour and Rizzano (2017) completed research on an energy dissipative steel angle holdown connector (XL-stub) fastened to opposing faces of a wood member using through-bolts. The testing was performed in a loading machine that provided axial loading to the upright leg of the connector and is shown in Figure 5. The horizontal leg in contact with the holdown anchor was reduced to an hourglass shape between the foundation anchor and the upright leg to force yielding in the steel plate prior to the wood fasteners.



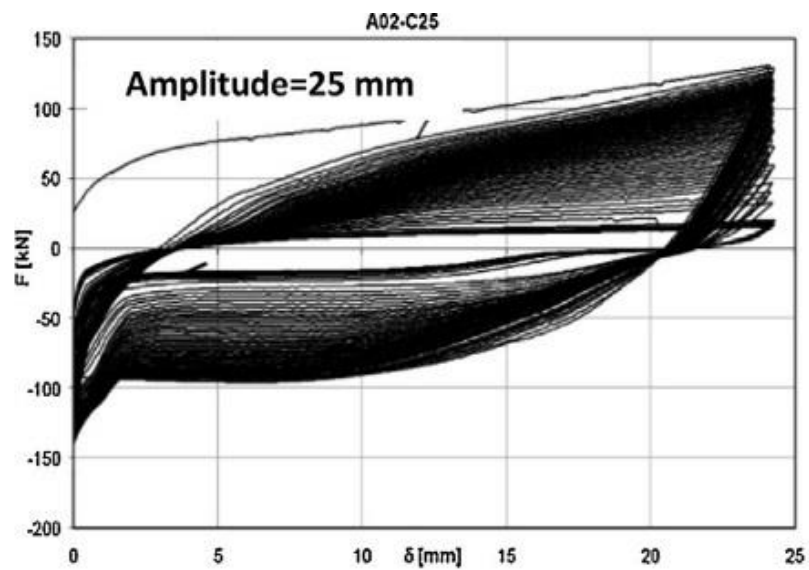
Figure 5 XL-stub holdown connections tests (Latour & Rizzano, 2017)

The reduced angle cross-section responded very well to cyclic loading. At a vertical displacement of 15 mm the XL-stub maintained half its energy dissipation

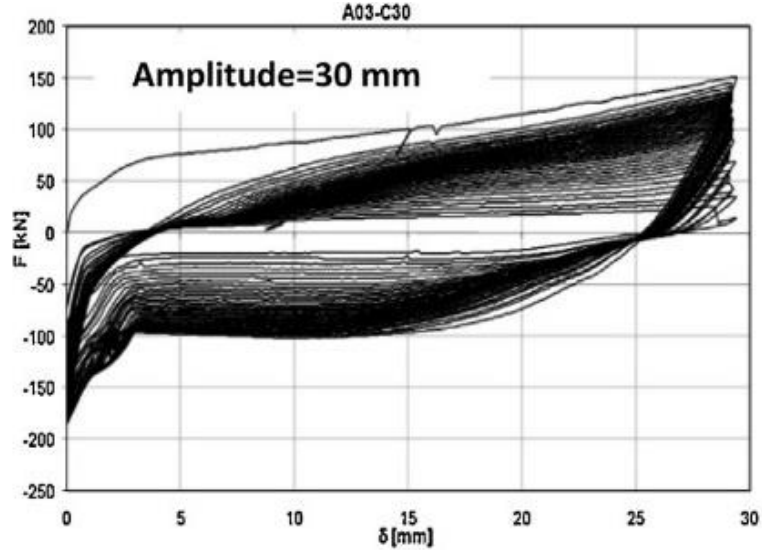
capacity following 100 cycles. At a higher amplitude of 30mm the holdown survived 29 cycles before reaching 50 percent energy dissipation capacity. The ultimate capacity of the connector ranged from 100 to 150 kN during the initial loading. The load-displacement response is shown in Figure 6 for three different amplitudes.



(a)



(b)



(c)

Figure 6 Load-displacement response of XL-stub (Latour & Rizzano, 2017)

The XL-stub is a good example of the ductility that can be achieved by using a weak-plate strong-fastener approach. The study did not include a shear wall assembly test using the holdown to verify the behavior under actual loading conditions. The XL-stub assembly used during testing would be required to face mount on opposing sides of the CLT panel to reach the measured capacities. While the connector displayed a robust hysteresis loop and high load capacities, this configuration would create architectural and fireproofing complications that a concealed connector would help resolve.

The research recently completed by Zhang, Popovski, and Tannert (2018) utilized steel connector plates and adhesives to achieve high-capacity knife-plate connections. The steel plate was perforated with 10 mm holes on a 15 mm grid and anchored to the panel through adhesive bonding. Tape was applied to one or two rows of perforations on the edge of the panel allowing the unbonded 5 mm links to provide a yielding

mechanism. The knife-plate connection assembly is shown in Figure 7. The plate thickness used was 2.55 mm, which required two 335 mm long plates in a seven-ply CLT panel to achieve higher load capacities. Full scale holdown tests were performed with the holdown assembly adhered to one side of the panel specimen.

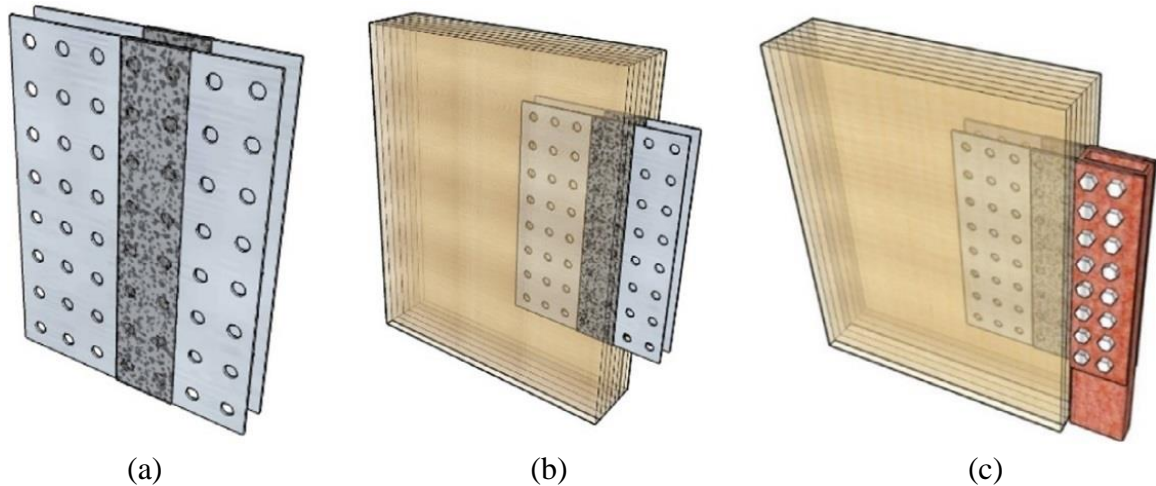


Figure 7 Adhesive knife plate connection setup (Zhang et al., 2018)

The perforated plates performed well under cyclic loading and experienced a ductile failure as indicated in the load-displacement response shown in Figure 8. This testing confirms that a more ductile connection can be developed by forcing the plate to yield and allows for a partially concealed connection. The ultimate capacities reached using the selected plate dimensions were approximately 170 kN with a yield strength of approximately 100 kN. This research provides a foundation for additional testing using thicker plates to achieve higher capacities and higher volumes of steel that yield in shear. The thicker plate and layout will allow for use of steel dowel fasteners and increased energy dissipation.

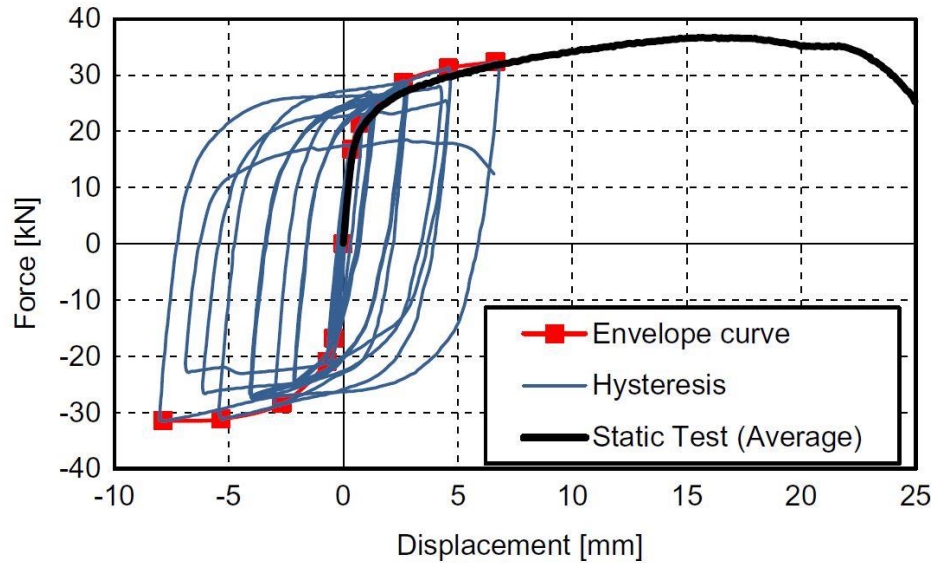


Figure 8 Adhesive holdown load-displacement response (Zhang et al., 2018)

Scope and Limitations

The purpose of this investigation was to expand upon the research summarized in this chapter and to develop a high-capacity ductile holdown connection that meets architectural and constructability constraints for CLT shear walls. The investigation consisted of exploratory testing to develop the holdown connection followed by a study of the strength and stiffness response of a CLT shear wall assembly utilizing the holdown connection.

The connection methods in this research utilize two configurations of steel knife plates as show in Figure 9, rather than conventional surface mounted steel hardware to form a double shear condition at each knife plate. The double shear condition takes advantage of a larger and more evenly distributed fastener bearing interface than a single

shear connection formed using surface mounted hardware. To obtain the targeted ultimate capacity of 75 kips each fastener failure mode needed to be optimized to limit the number of fasteners required.

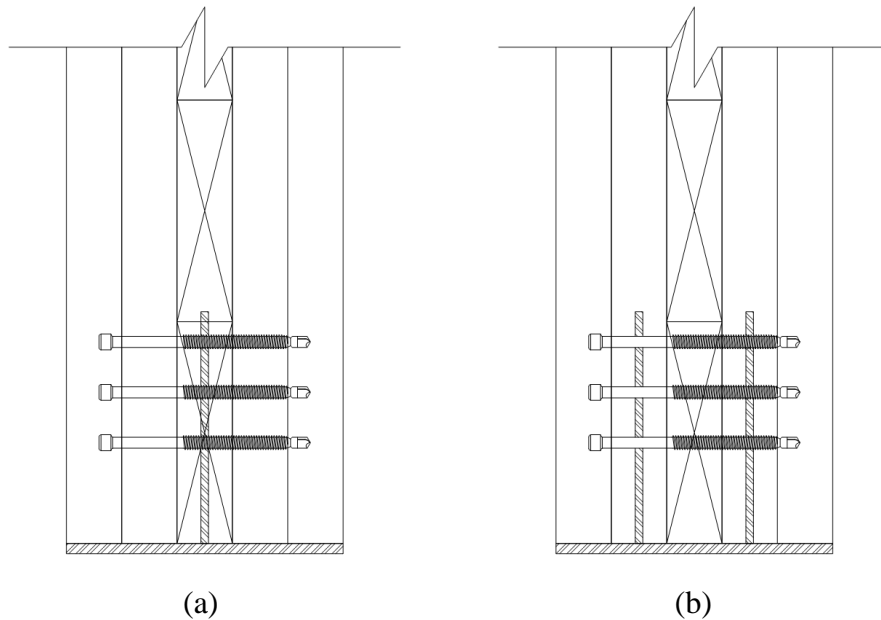


Figure 9 Knife plate configurations

The exploratory testing began with shear and bending tests to determine the fastener properties. The subsequent tests utilized single and double knife plate configurations to establish the preferred layout for the knife plate and fasteners. Once the knife plate quantity and thickness were determined, finite element analyses (FEA) were conducted to optimize the layout for the reduced section of the knife plate forming the ductile yield zone. Steel plate testing was conducted to validate the result from the FEA model. The holdown configuration was then assembled using the results from the fastener and steel plate testing.

The final tests utilized a CLT shear wall specimen and the developed holdown connection to study the behavior of the lateral-force resisting system. The holdown assembly was installed on the panel and anchored to the strong floor allowing the panel to resist cyclic lateral loading. The holdown and panel responses were recorded to try to determine the system performance.

EXPERIMENTAL PROGRAM

Materials

The materials utilized for this research consisted of steel fasteners, CLT panels, and steel plate. The fasteners were provided by MyTiCon Timber Connectors, a heavy and mass timber connection supplier located in Surrey, BC. The CLT panels were provided and manufactured by Smartlam, a CLT manufacturer in Columbia Falls, MT. The plate material was grade 36 steel provided by True Cut Laser, who also used laser and plasma cutting to fabricate the reduced-section plates designed for the small- and full-scale tests of this experimental program.

Self-Drilling Dowel

The self-drilling dowels (SDD), MyTiCon item numbers 360070133000808 and 360070153000808, were manufactured with a partial-length mild thread pattern intended for cutting into metal to help drive the dowel through the connection and hold the fastener in place. The screws can be used in a variety of timber connections to secure steel knife plates in a surrounding member as shown in Figure 9. A tight fit is developed as the screw cuts through each material reducing connection slip and making it ideal for the intended holdown connection. The screw tip self-drills through wood and harder materials such as steel. However, for steel thicknesses greater than 0.125 in. and multiple plate connections predrilling was necessary for easier installation. The installation torque for the fasteners is low allowing for simple field installation using cordless drills. The concealable dowel head uses an AW 40 bit to drive the fastener providing a small

diameter hole that is easy to plug for a fire rated connection. A design guide for the SDD fasteners (MyTiCon Timber Connectors, 2019) was recently published by MyTiCon Timber Connectors that contains necessary design values for current wood design codes within the United States. A photograph of the fasteners is shown below in Figure 10.



Figure 10 Self-drilling dowel

The steel fasteners used for testing were 5.25 in. and 6 in. in length and 0.25 in. in diameter and were fabricated using SAE/ANSI 1018 material. The fastener lengths were selected for compatibility with the CLT specimens. The material used for the fasteners provides a high bending strength that allows the load to distribute more evenly across the length of the fastener in a knife plate application and provides a stiffer connection. The fastener material properties are included in Table 1 below.

Table 1 Fastener Material Properties

MyTiCon Design Guide Values (MyTiCon Timber Connectors, 2019)	
Bending Yield Strength (F_{yb})	126,200 psi
Allowable Shear Strength	1725 lbs.
SAE/ANSI 1018 Material Properties (AZoM, 2012)	
Elastic Modulus	29,700 ksi
Ultimate Tensile Strength	63,800 psi
Yield Strength	53,700 psi

CLT Panels

Smartlam CLT panels are manufactured using No. 2 Spruce-pine-fir (SPF) or Hem-fir (HF) dimension lumber glued together in a variety of layups in accordance with PRG320-18 (American Plywood Association, 2018b). The CLT panels used for testing were a 5-maxx HF layup containing two outer plies on each side oriented parallel to each other and one orthogonal center ply as shown in Figure 11. The more typical panel configuration is a 5-alt layup with each of the five plies oriented orthogonally to the adjacent plies as shown in Figure 12, however, this layup was not used for testing in this project. Each ply is assembled using nominal 2x6 sawn lumber sanded to 1.375 in. forming a 5-ply panel thickness of 6.875 in. Smartlam CLT panels can come in widths ranging from 12 to 120 inches and lengths up to 40 feet. The design properties for Smartlam CLT panels can be found in the APA Product Report PR-L319 (American Plywood Association, 2018a).

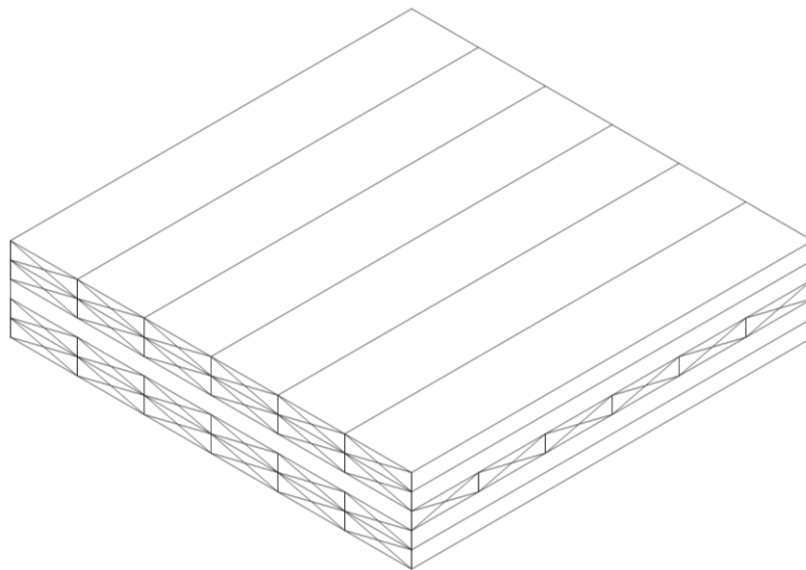


Figure 11 5-maxx CLT panel

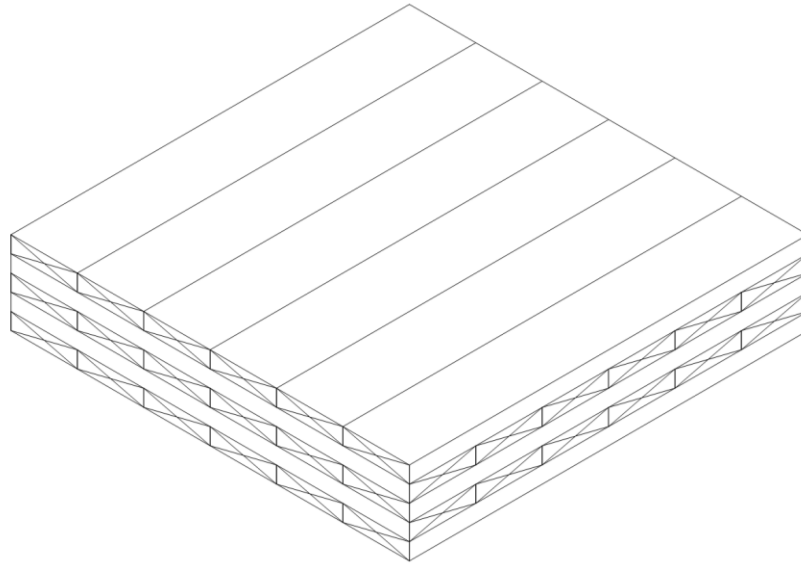


Figure 12 5-alt CLT panel

CLT panels are typically used for roof, floor, and wall applications in buildings. The panels are very stiff allowing for rigid diaphragm analyses and more slender shear wall segments than light framed wood shear walls. CLT is ideal for prefabricated structures due to potential size of each panel and the advanced milling and modeling techniques available to manufacturers and designers. Typically, panels are cut by the manufacturer with large CNC machines using computer automated drawings from a designer. This process requires that the structure be completely designed prior to manufacturing but allows for faster and more accurate cutting and installation of the panels to increase on-site efficiency during construction.

Steel Plates

The steel plates used for testing were grade 36 steel. The steel grade and thicknesses selected are readily available throughout the United States. The single knife

plate tests were performed with 0.25 in. thick plate, while the double knife plate tests were performed with two 0.112 in. thick plates. The mild steel provides a reliable and ductile response to cyclic loading as historically demonstrated in structural steel design. Similar tactics to those used in braced frame and moment frame design are employed in this project to force the system failure to occur in a desired location that will not result in a brittle failure.

Small-Scale Exploratory Tests

Initial testing performed during this investigation was chosen to develop a holdown connection suitable for achieving a ductile response at a targeted ultimate capacity of 75 kips. Single and small groups of fasteners were tested to determine a knife plate configuration and fastener layout with a working capacity equivalent to the targeted load. Steel plate testing and modeling was performed to develop a steel knife plate with a reduced section that would provide the desired response at approximately 75 kips. All exploratory testing was performed using a 1000 kN MTS Static-Hydraulic Universal Test Frame.

Fastener Bending and Shear Tests

Direct bending tests were performed in accordance with ASTM F1575 (ASTM International, 2008). The standard specifies a three-point load test with a span between supports equal to 11.5 times the fastener diameter for fastener diameters larger than 0.190 inches. The bending test setup can be seen in Figure 13. The maximum load rate specified by the standard is 0.25 inches per minute. The load rate used for the bending

tests was 0.24 in. per minute and the bearing length between supports was 3.068 in. as shown in Figure 14. Eight iterations of the direct bending tests were performed.

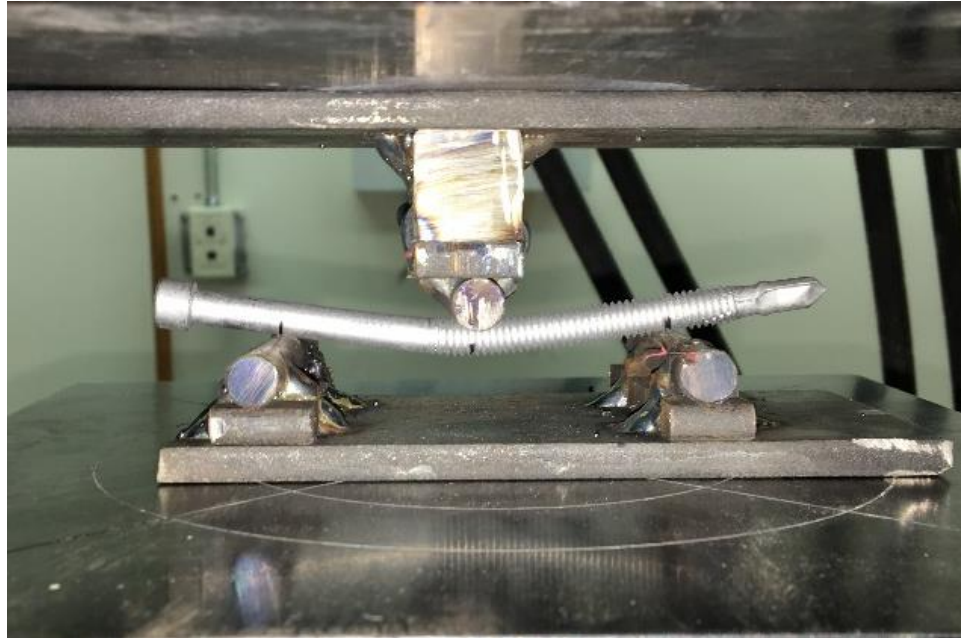


Figure 13 Fastener bending test setup

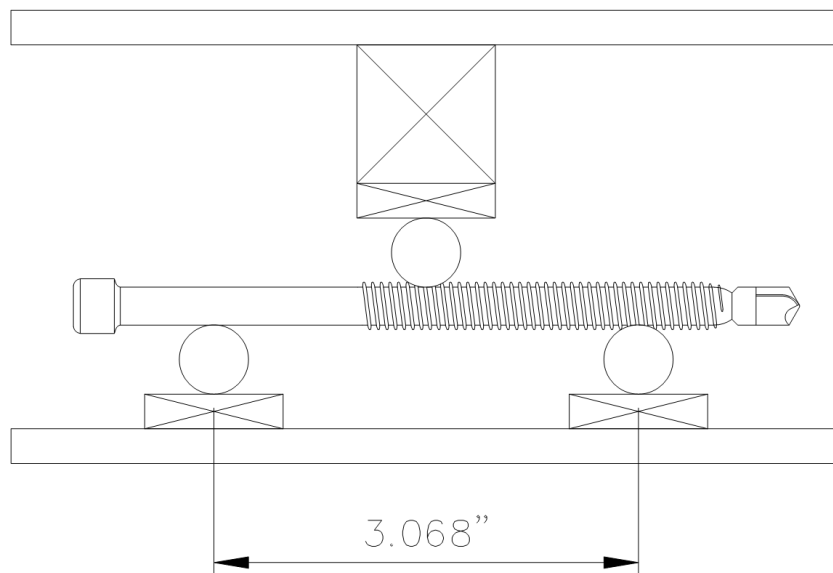


Figure 14 Fastener bending test layout

Fastener shear testing was performed in accordance with AISI TS-4-02 (American Iron and Steel Institute, 2001) but in a double shear condition to determine the shear strength of the fasteners. The test setup for the shear tests can be seen in Figure 15 below. The test setup utilized three pieces of 1 in. square steel stock with a 0.25 in. diameter semi-circle drilled into each member as shown in Figure 16 to form a uniform bearing surface with the fastener. The load rate used for the test was 0.59 in. per minute. Seven iterations of the fastener shear tests were performed.

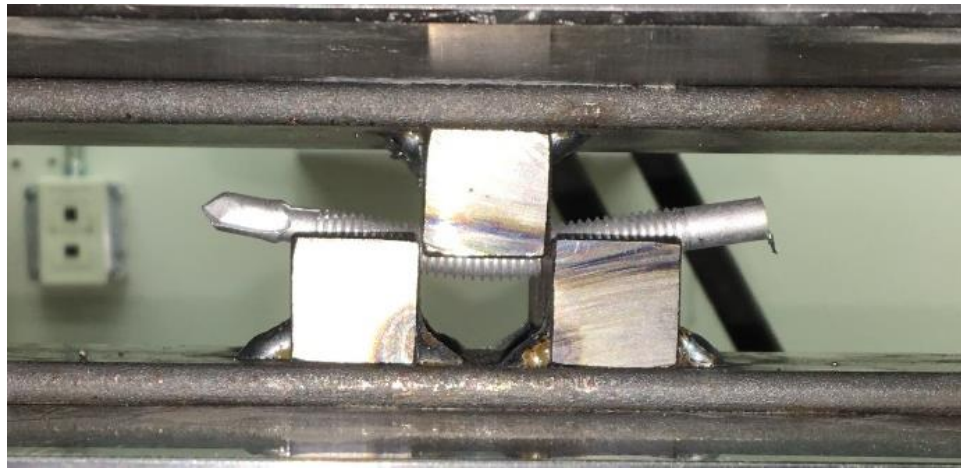


Figure 15 Fastener shear test setup

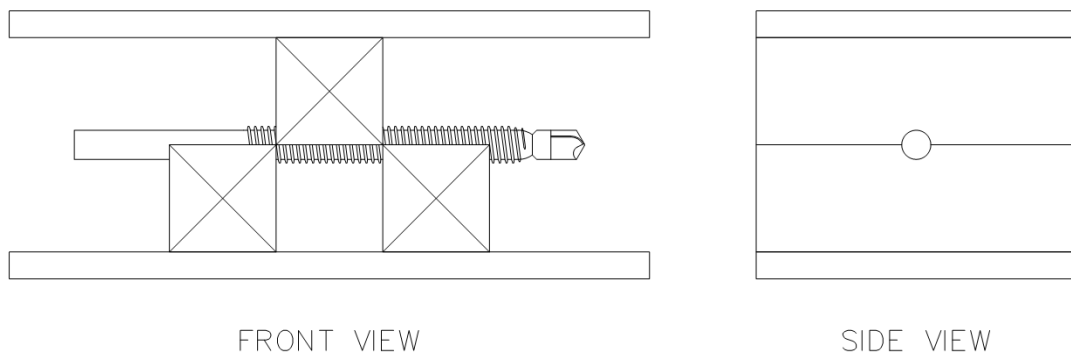


Figure 16 Fastener shear test layout

Single Knife Plate Tests

The initial connection tested utilized a single 0.25 in. thick knife plate in the center ply of a CLT specimen. The connection geometries and fastener layouts for the single and group tests are shown in Figure 17 and Figure 18. The knife plate tests were performed in accordance with ASTM D 5764 – 97a (ASTM International, 2002) but using the single knife plate configuration in tension loading rather than the double shear compression test in the standard. The assembled test specimens for the single and group fastener tests are shown in Figure 19a and Figure 19b. The CLT specimens were cut into approximately 10x14 in. samples to allow for adequate edge and end distances for the threaded fasteners. A chain saw was used to cut the knife plate opening measuring approximately 0.3x4.5 in. through the center ply of each sample. Steel knife plates were installed on opposite ends of each sample using a substantially stronger connection on one side to induce failure of the connection geometry under investigation.

The fasteners used for the single knife plate tests were 0.25x5.25 in. SDD fasteners. The single fastener tests were performed using a ‘strong-end’ connection of six fasteners and a single fastener on the opposite end moving towards the edge of the panel for each test. Three iterations of the single fastener tests were performed using each panel specimen as indicated with the grey fasteners in Figure 17. The second test configuration replaced the single fasteners with four 0.75 in. diameter bolts for the ‘strong-end’ connection in order to investigate the group action effect of the six SDD fasteners used previously. The knife plates were installed in the specimen such that the fasteners loaded the CLT specimen perpendicular to grain at the shear plane. The group fastener test

configuration is shown in Figure 18 and photographs of the two test configurations are shown in Figure 19.

The single knife plate assemblies were tested using the MTS test frame to determine the monotonic load-displacement curve for each test configuration. The load rates used for the single knife plate tests were 0.1 in. per minute for the single fastener tests and 0.2 in. per minute for the group fastener tests. The load rates were selected to reach the maximum load in less than 10 minutes per ASTM D 5764 – 97a (ASTM International, 2002). Six iterations using a single and a group of fasteners were completed.

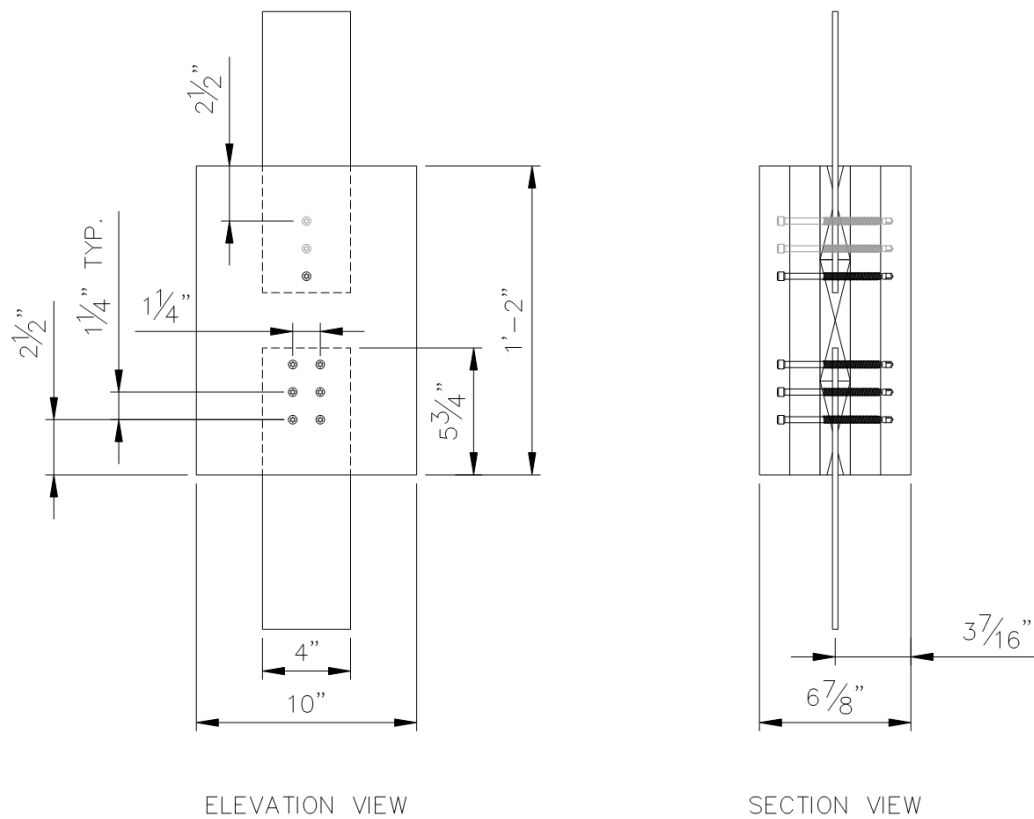


Figure 17 Single knife plate single fastener test layout

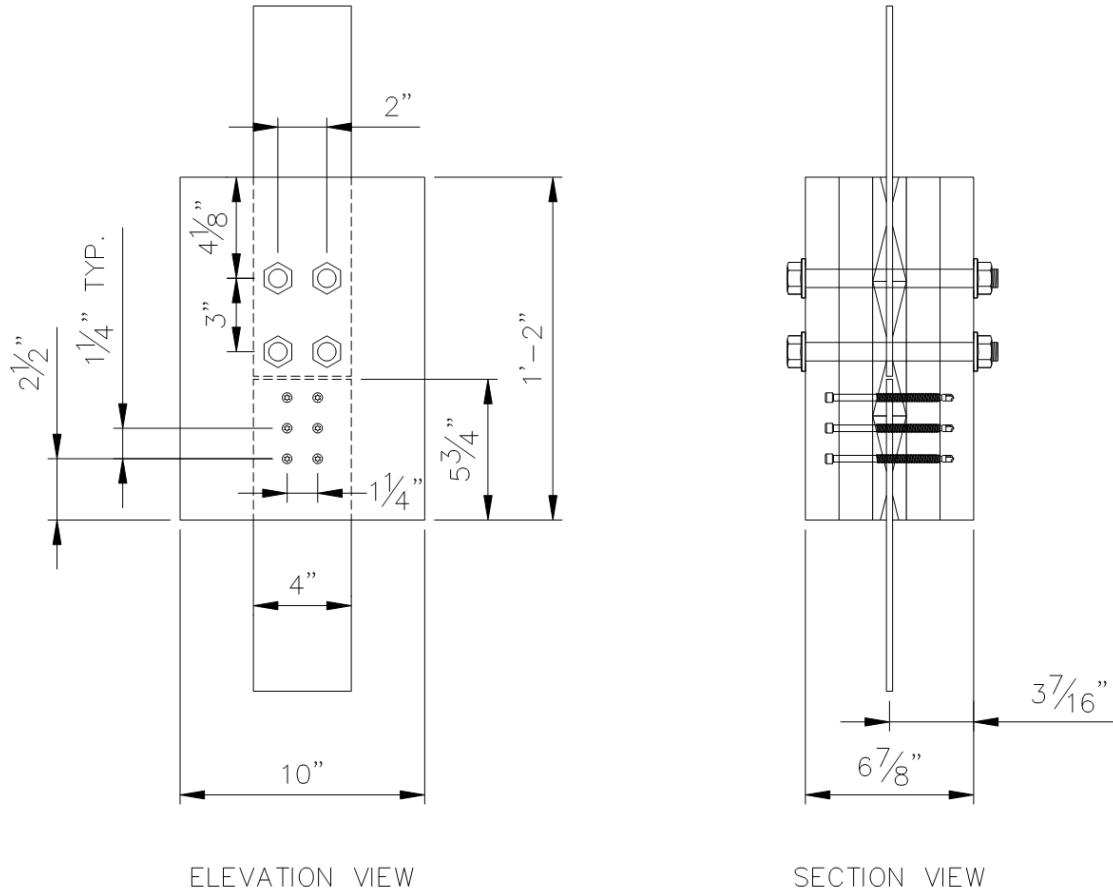


Figure 18 Single knife plate group fastener test layout

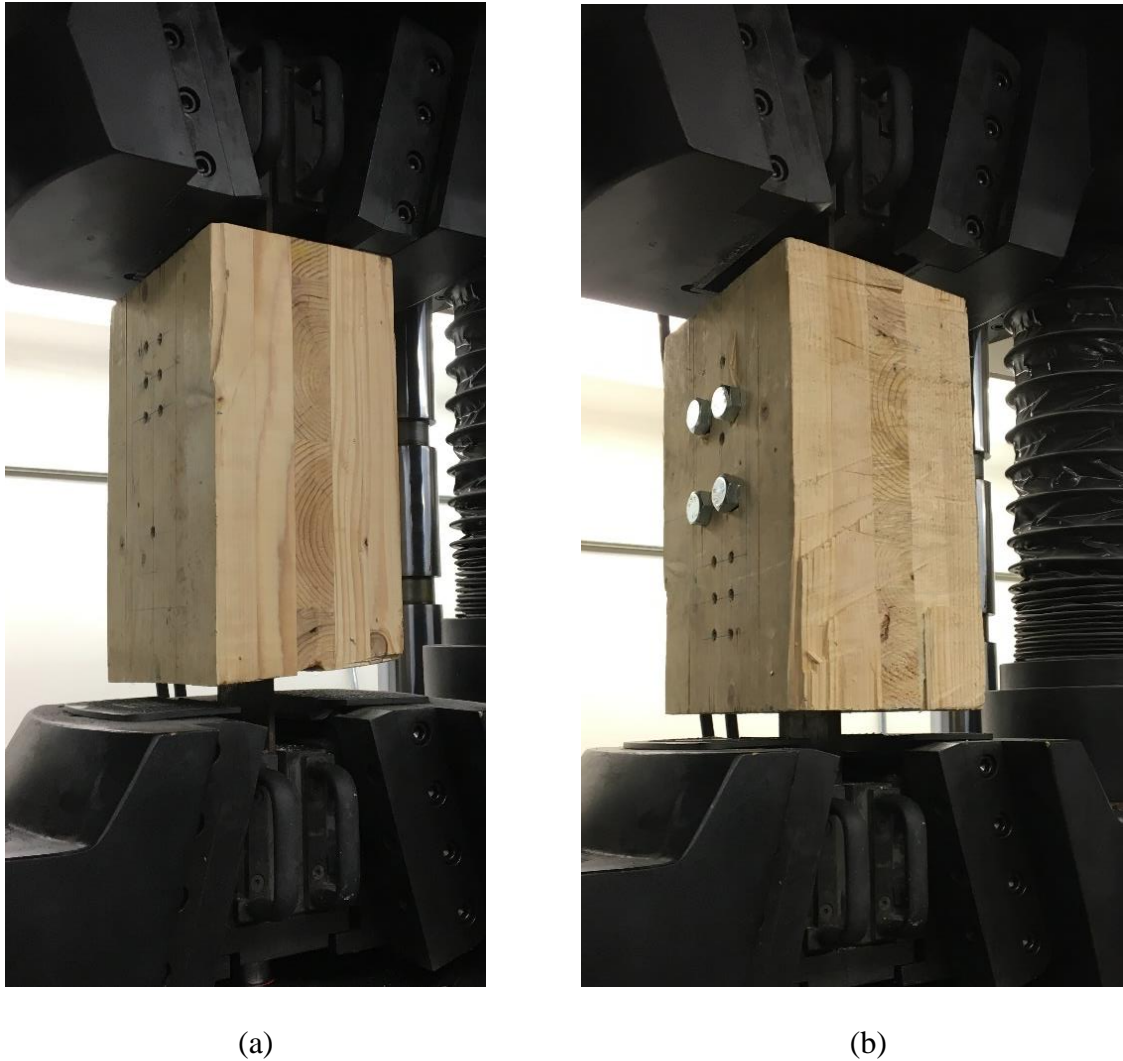


Figure 19 Single knife plate test setups

Double Knife Plate Tests

The second connection tested used two 0.112 in. thick knife plates spaced 2.75 in. apart to increase the stiffness and capacity of the connection. The double knife plate test setups were fabricated to create a geometry that could be tested in the MTS test frame. The CLT specimens were cut into approximately 8x14 in. samples with two knife plate openings measuring approximately 0.25x3.5 in. through the second and fourth plies of

the panel. The fasteners used for the double knife plate tests were 0.25x5.25 in. SDD fasteners. The SDD fastener configurations mimicked the layouts used for the single knife plate tests and are shown in Figure 20 and Figure 21. The knife plate tests were performed in accordance with ASTM D 5764 – 97a (ASTM International, 2002) but using the double knife plate configuration in a tension test assembly. The assembled test specimens for the single and group fastener tests are shown in Figure 22a and Figure 22b. The knife plates were installed in the specimen such that the fasteners loaded the CLT specimen parallel to grain at the shear planes. The load rate used for the double knife plate tests was 0.13 in. per minute for both the single fastener tests and the group fastener tests. The load rate was selected to reach the maximum load in less than 10 minutes per ASTM D 5764 – 97a (ASTM International, 2002). Six iterations of each tests were performed.

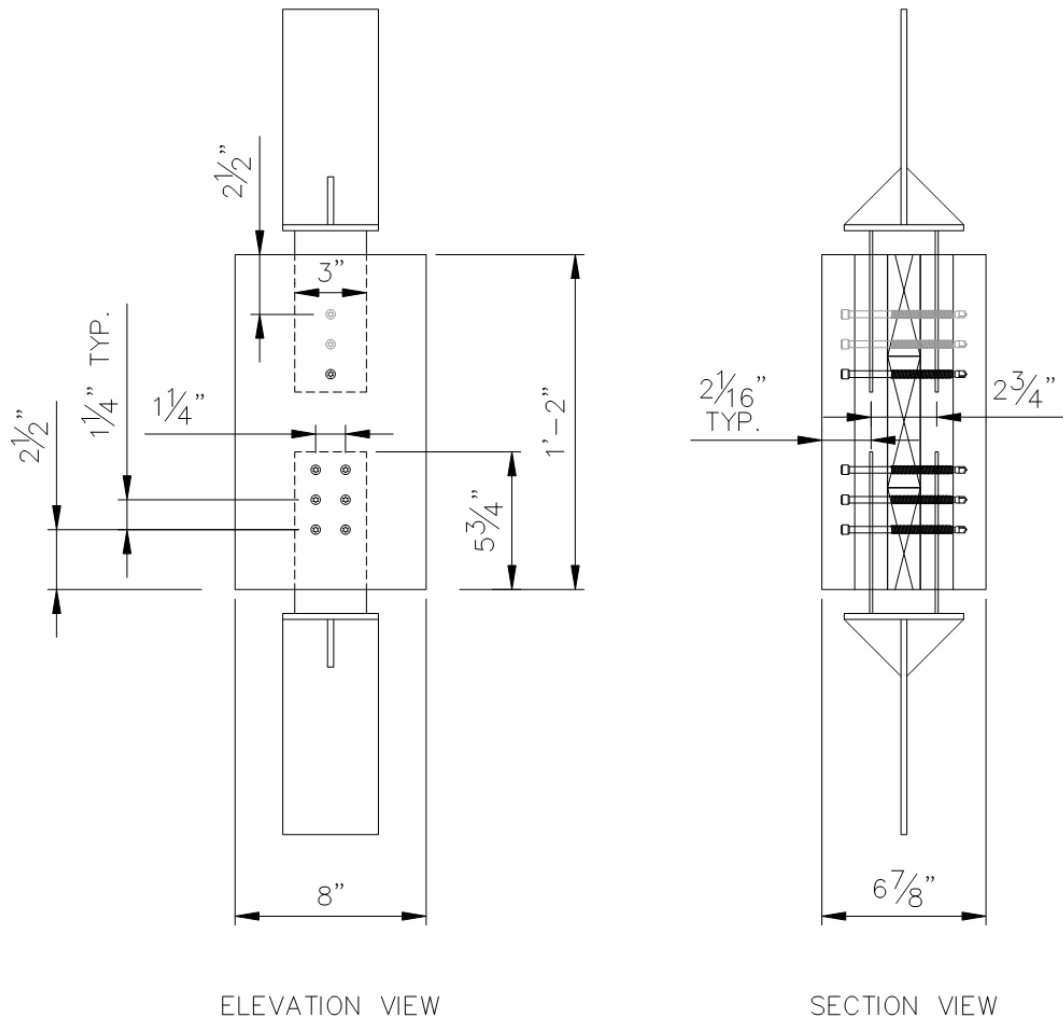


Figure 20 Double knife plate single fastener layout

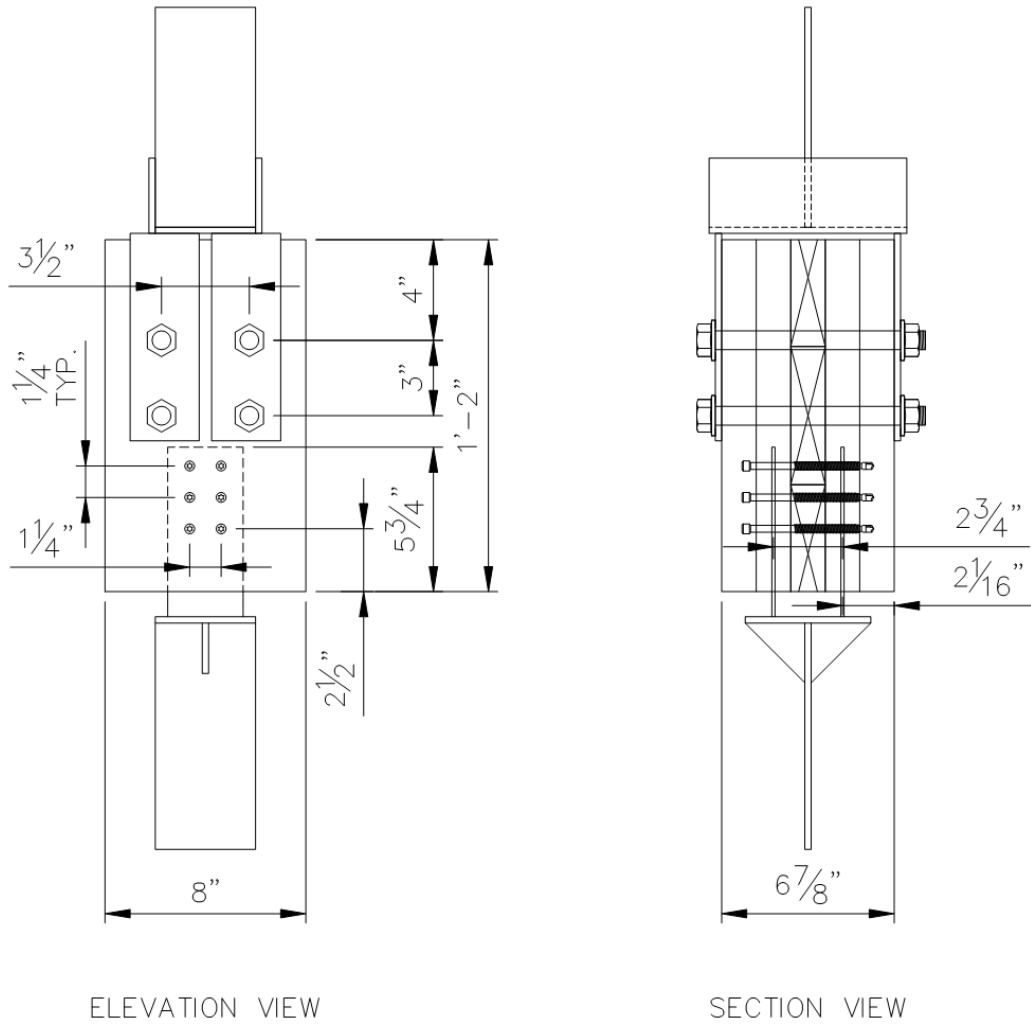


Figure 21 Double knife plate group fastener layout

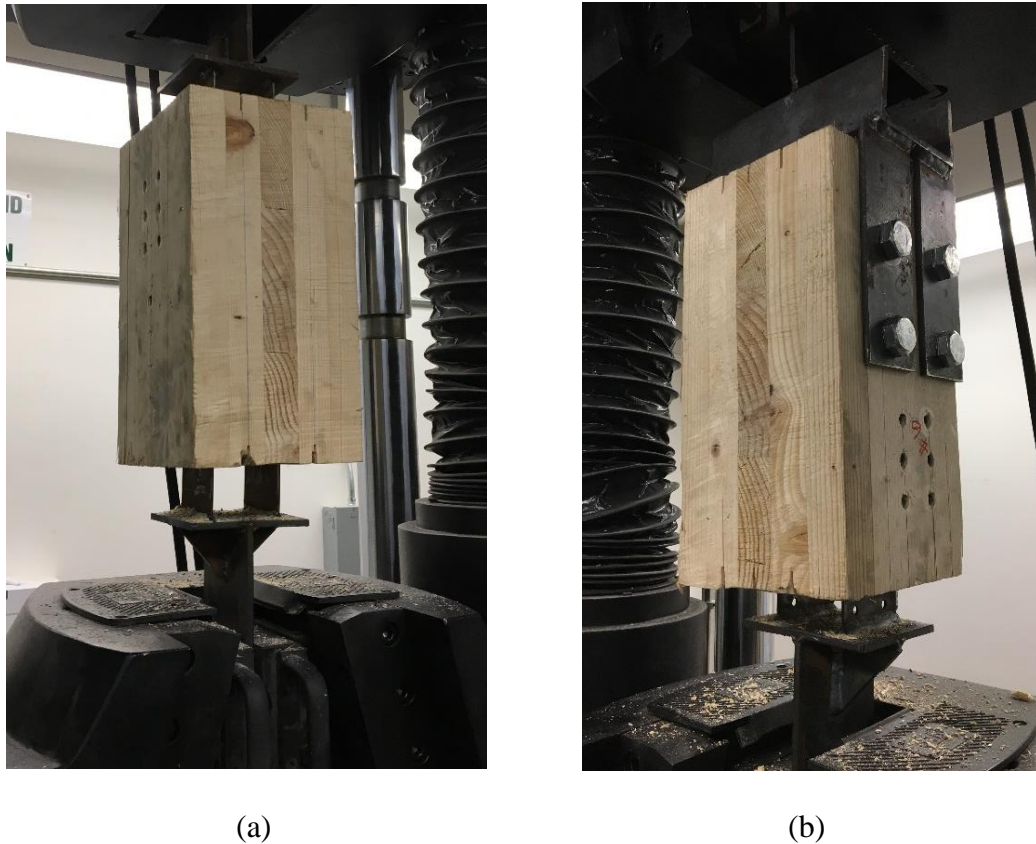


Figure 22 Double knife plate tests setups

Reduced Section Steel Plate Modeling

Following the wood connection testing a reduced section knife plate was designed using FEA models to develop a ductile yield zone in the knife plate prior to reaching the group fastener capacity. The reduced section is intended to provide reliable energy dissipation through successive yielding of the steel plate rather than permitting substantial crushing of the CLT panel or large displacement yielding of the fasteners. The desired layout for the reduced section was applied to a preliminary small-scale reduced section steel plate that could be tested in the MTS test frame to validate the FEA model prior to completing the plate design for the full-scale holdown connections. The

goal of the final reduced section layout was to provide a large volume of steel reaching the plate yield stress at the desired deflection and targeted load for assembly.

The preliminary FEA modeling included a variety of patterns for the reduced section of the steel plate. The deflection range used for modeling was increased incrementally between 0.1 and 0.5 inches based on allowable drift limitations set forth in ASCE7-10 (American Society of Civil Engineers, 2010) for a one-story panel including approximate panel deflections and fastener slip. On the side of the steel plate that would be welded to the holdown anchorage plate, all rotational and displacement degrees of freedom were fixed. On the opposite side of the plate where vertical displacements were applied only the out-of-plane displacement degree of freedom was fixed.

The analytical modeling was performed in ANSYS using eight-node quadrilateral SHELL281 elements to model a grade 36, 0.112 in. thick hot rolled steel plate. The small-scale steel plates were meshed using elements with a maximum element size of 0.03125 in. in an isotropic bilinear hardening model using nonlinear geometry. The number of elements used was determined through a stress contour plot convergence study. The elastic modulus used for the models was 29,000 ksi and the tangent modulus used was 965 ksi. The tangent modulus was selected to provide an equivalent amount of energy dissipation within the applicable portion of the stress-strain curve.

Reduced Section Small-Scale Steel Plate Tests

The small-scale reduced section steel plates were fabricated using a CNC laser cutting machine with grade 36 11-gauge ASTM A1011(04A) type B hot rolled steel and were loaded using the MTS test frame to validate the FEA model. The test set up used for

the reduced plate testing and FEA is shown in Figure 23. As shown using the grey hatch pattern, 0.25x3 in. steel stiffener plates were welded to each small-scale reduced section plate to mimic the conditions of the holdown assembly and provide a uniform load distribution to the yield zone. The reduced section steel plates were subjected to monotonic load tests to validate the results of the FEA model as shown in Figure 24. The plates were not loaded cyclically to determine the fatigue response and obtain hysteresis loops due to limitations of the static test frame assembly used. The load rate used for the monotonic tests was 0.1 in. per minute and the specimens were loaded to a maximum total vertical displacement of 1.3 in.

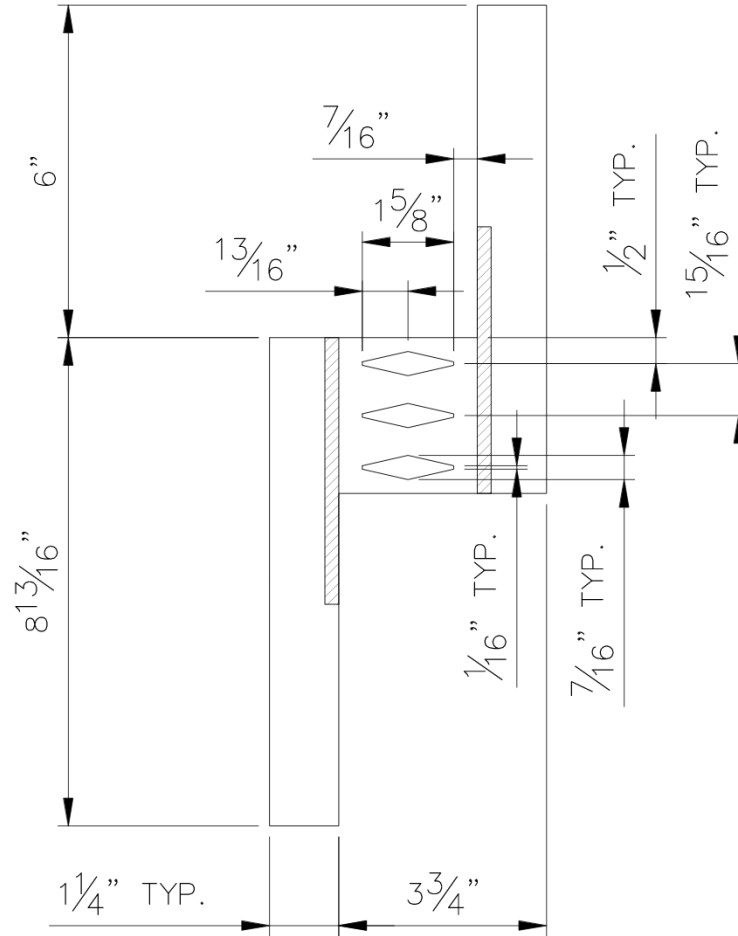


Figure 23 Small-scale reduced section plate layout

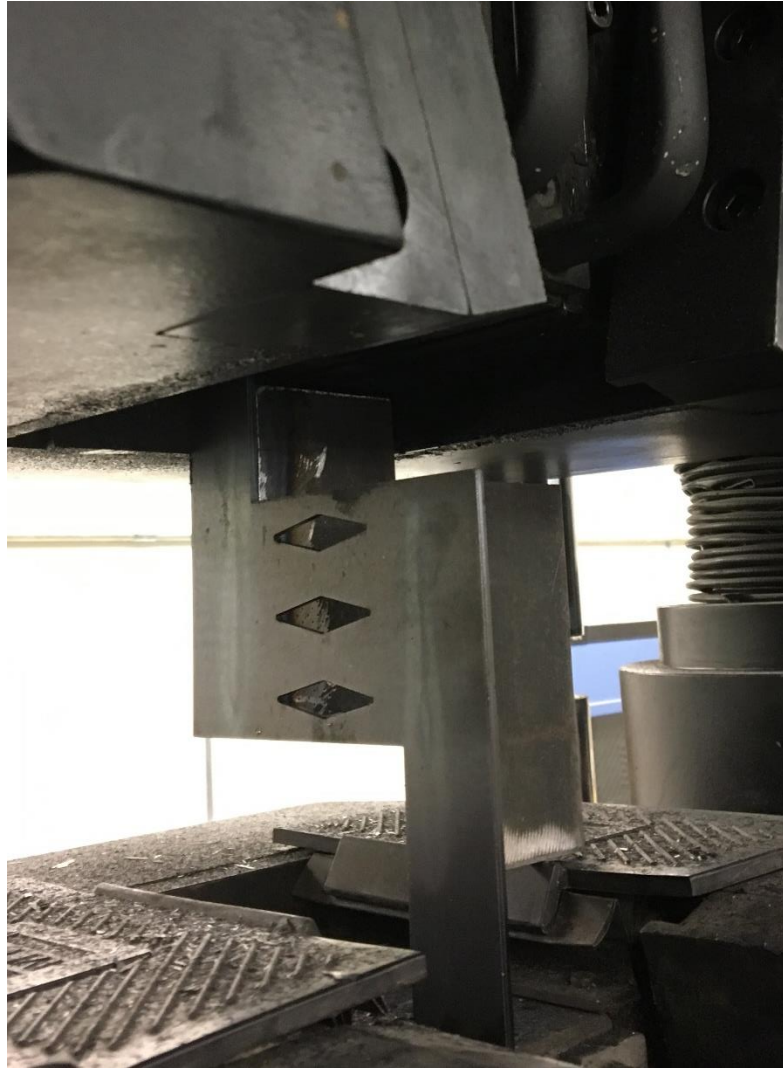


Figure 24 Small scale reduced section test assembly

CLT Shear Wall Test

The final testing utilized data acquired during the fastener and steel plate exploratory tests to design a shear wall assembly that would provide high lateral load capacities and increased cyclic ductility. Using the validated small-scale FEA steel plate model the reduced section for the larger steel knife plates was scaled to the layout shown

in Figure 25 to yield at a targeted ultimate capacity of 75 kips and a deflection of 0.3 in. The steel plate yield displacement of 0.3 in was intended to provide an approximate total lateral deflection of 0.7 in. for a 3x10 ft CLT panel after incorporating additional displacement from the fastener slip and panel deflection. The load-displacement response from the double knife plate group fastener tests was used to determine the fastener layout for the full-scale holdown connection at approximately one half the ultimate capacity when accounting for a 0.9 group action factor (C_g) and a fastener connection displacement of 0.14 in. A full-scale holdown assembly using two reduced section steel plates at each holdown was assembled and tested to determine the system behavior under lateral loading. The reduced section steel plates were fabricated using a CNC plasma cutting machine with grade 36 11-gauge ASTM A1011(04A) type B hot rolled steel. The dimensions of the steel knife plates were selected to allow for practical fabrication of the CLT panel while maintaining proper spacing for the required number of fasteners. The reduced section of the steel knife plates was designed to obtain the chosen yield load at a targeted displacement. The larger knife plates were designed using a similar ANSYS model to the small-scale steel plates but with a maximum element size of 0.0625 in. based on convergence of the Von Mises element stress plot. The CLT shear wall assembly layout is shown in Figure 26.

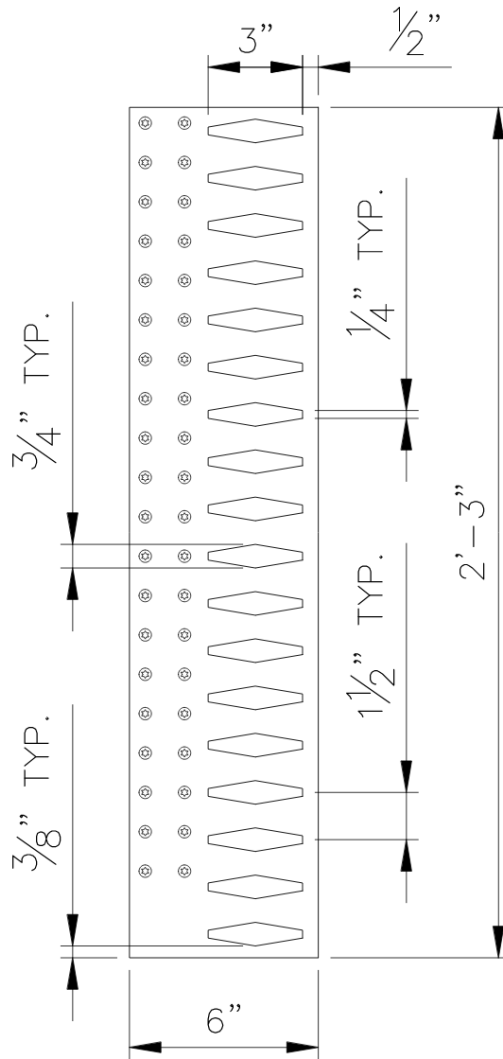


Figure 25 Full-scale reduced section plate layout

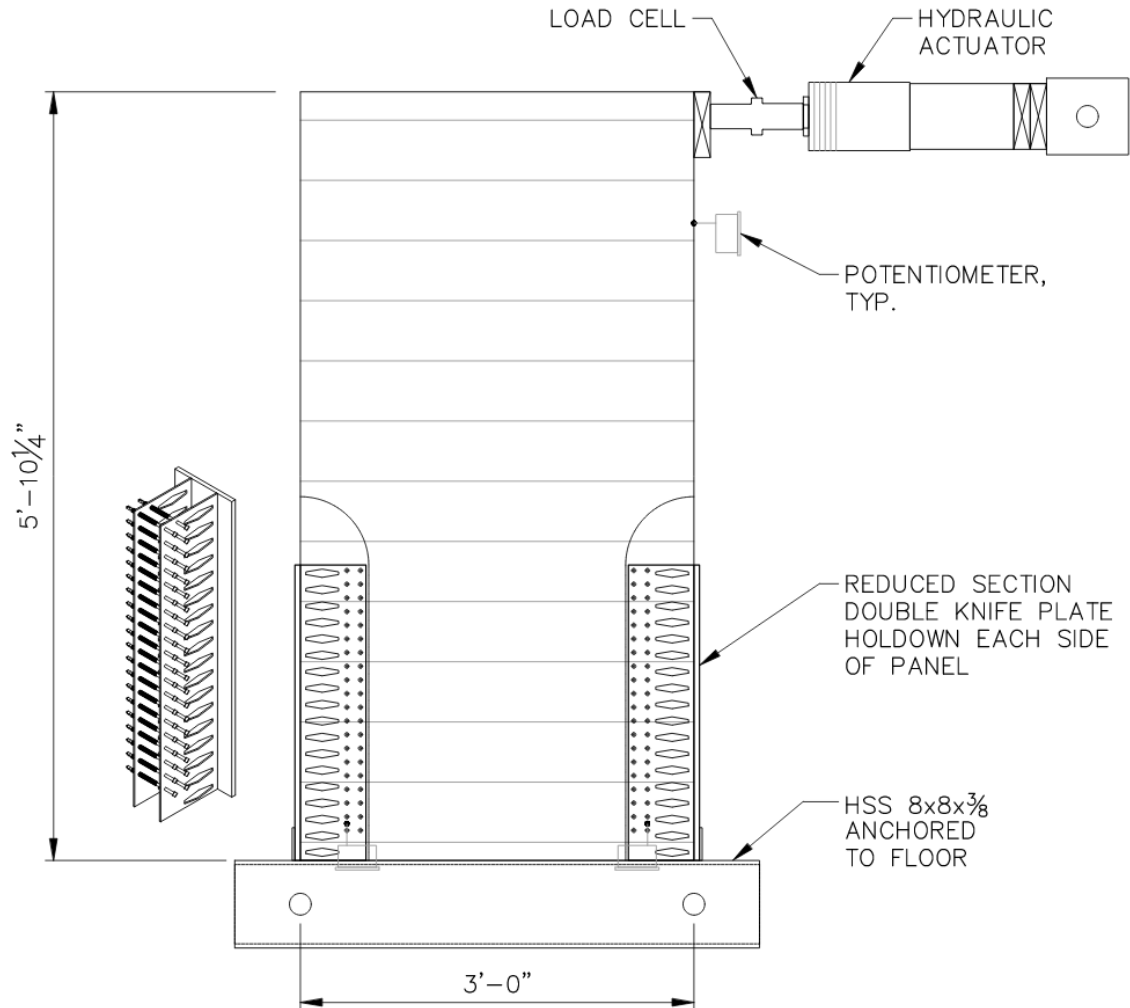


Figure 26 CLT shear wall assembly layout

The 6 in. width of the knife plates was selected for compatibility with a 16.3125 in. circular saw to cut the knife plate slot in the panel, however, for this project a chainsaw was used to cut approximately 0.25 in. wide slots in the second and fourth plies of the specimens as shown in Figure 27. The holdown assembly utilized a 0.375x6 in. A36 plate along the side of the CLT panel to anchor the holdown to the 8x8x0.375 in. hollow structural shape (HSS) as shown in Figure 28. The reduced section knife plates

were welded to the side plate as shown in Figure 28, but were left unconnected at the base to the steel tube. This allowed the portion of the plate with the fasteners through it to displace vertically, thereby forcing the plates to yield when subjected to the targeted uplift force. Each holdown utilized 40 SDD fasteners through two knife plates that were spaced 2.75 in. apart. The fasteners used for the shear wall assembly were 0.25x6 in. SDD fasteners spaced 1.25 in. apart with a 0.5 in. steel plate edge distance.



Figure 27 Full-scale knife plate slots



Figure 28 Full-scale holdown assembly

The shear wall test setup was intended to be subjected to 4 load cycles, however, only 1.5 cycles were completed before reaching the ultimate capacity of the test setup. The shear wall assembly had been designed to incorporate a 3x10 ft CLT panel, but due to material delays, was adapted to a 3x5.9 ft panel. The reduced panel height required a larger applied lateral load to obtain the desired 75 kip uplift force on the holdown connection and caused instability of the hydraulic cylinder, load cell and spacer

assembly. In addition, the available resources for this project and timeline did not allow for an out-of-plane restraint system to be applied to the CLT panel. The effects of this out-of-plane movement are expanded on in the results.

The CLT panel used in the shear wall assembly was a 5-maxx layup (Figure 11). The panel was oriented opposite of the fastener tests with the exterior plies running horizontally across the panel. Although the fasteners loaded the CLT specimen perpendicular to grain at the shear planes, the anticipated fastener load capacity was equivalent to the double knife plate group fastener tests due to the middle ply of the 5-maxx panel having a larger bearing capacity where the maximum fastener bending stiffness and load distribution occurs, the small diameter of the fasteners, and the increased length of the fasteners used for the shear wall tests.

Once the holdown assembly was installed on the CLT panel, the 8x8x0.375 HSS member at the base of the assembly was anchored to the strong floor using a 2 in. diameter bolt on one side and a 1.25 in. diameter Dwyidag bar post-tensioned to the strong floor on the opposite side. The smaller diameter Dwyidag bar was used to accommodate the misalignment of the holes in the HSS member and strong floor. Potentiometers were installed at each of the holdowns to measure vertical panel displacements and one potentiometer was installed at the top of the panel to measure lateral displacements. Additional potentiometers would have been useful to measure the lateral displacements at the base of the panel. The lateral loading reactions at the top of the panel were achieved by post-tensioning an assembly of four 7x7.5x2 in. steel plates to the strong floor using a 1.25 in. diameter Dwyidag bar. A SPXFLOW RH603 cylinder

jack was used to apply lateral load to the shear wall assembly on alternating sides of the panel to complete a full cycle. The completed shear wall assembly can be seen in Figure 29.



Figure 29 CLT shear wall assembly

RESULTS & DISCUSSION

Small Scale Exploratory Tests

Fastener Bending and Shear Tests

Direct bending tests were performed to determine the bending yield strength of the SDD fasteners to allow for application of the yield limit equations included in the National Design Specification for Wood Construction (NDS) (American Wood Council, 2017). The yield limit equations use the bending yield strength to determine the predicted failure mode for various connection geometries as summarized in Appendix I of the specification. The connection yield modes used in the NDS are shown below in Figure 30. The applicable yield modes for the connection configurations used in this research are the double shear configurations shown on the right side of Figure 30.

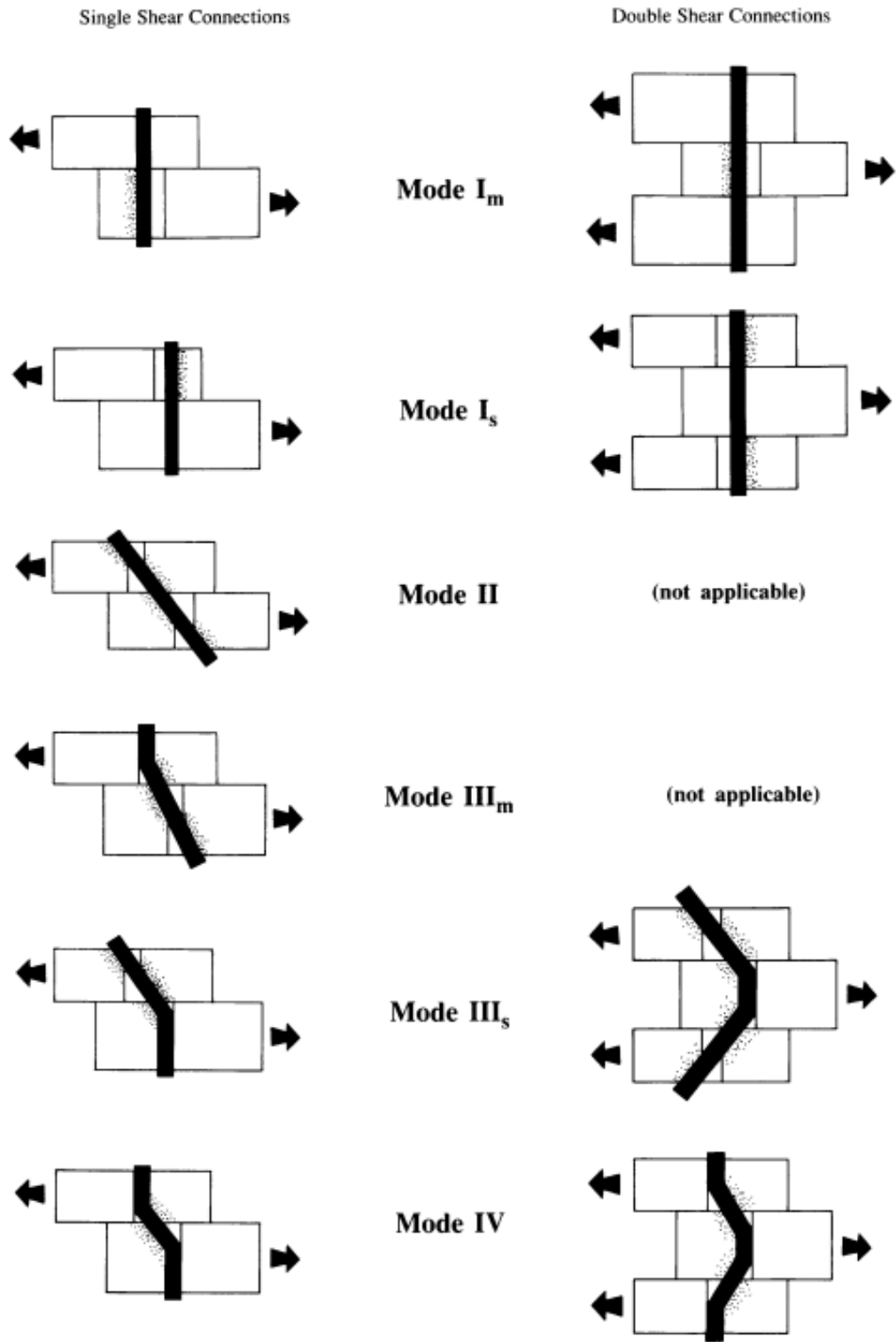


Figure 30 NDS connection yield modes (American Wood Council, 2017)

The bending yield moment used in the yield limit equations is determined by offsetting a straight line from the initial linear portion of the load-deformation curve by 5 percent of the fastener diameter as shown in Figure 31. The load value where the offset line intersects the load-displacement curve is used to determine the bending yield moment for each test run and averaged to provide a design bending yield moment for the fastener. The fastener root diameter used to calculate the plastic section modulus was 0.2645 in. This method was used to validate the MyTiCon published bending yield strength of 126,200 psi. The SDD bending test results and 5% offset values can be found in Table 2. The load-displacement curves for the eight tests used to determine the bending yield strength are shown in Figure 32 below. The dashed line indicates the approximate 5% offset used to determine the bending yield strength of the fasteners.

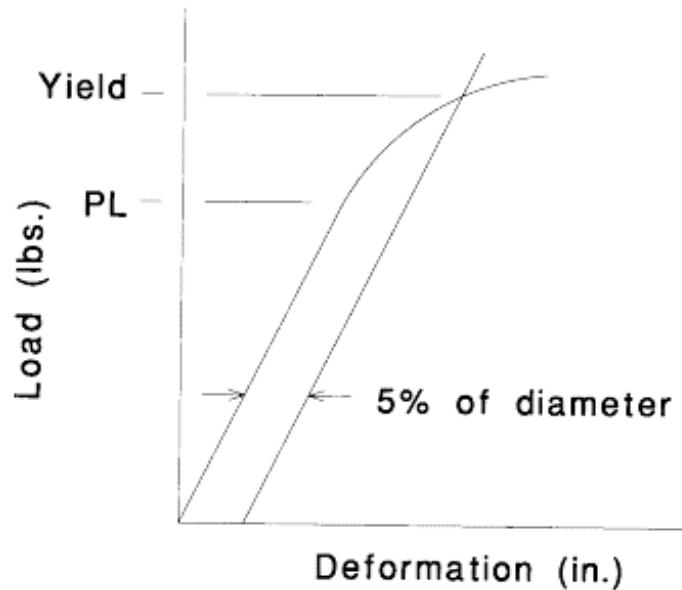


Figure 31 Load-deformation diagram for bending test (ASTM International, 2008)

Table 2 SDD Bending Test Results

Bending Test Results		
Test Number	Maximum Load (lbs)	Approximate 5% Offset (lbs)
Test #1	732	530
Test #2	752	535
Test #3	726	535
Test #4	763	545
Test #5	743	545
Test #6	531	350
Test #7	755	555
Test #8	690	460
Average	711	507
COV	10.8%	13.8%

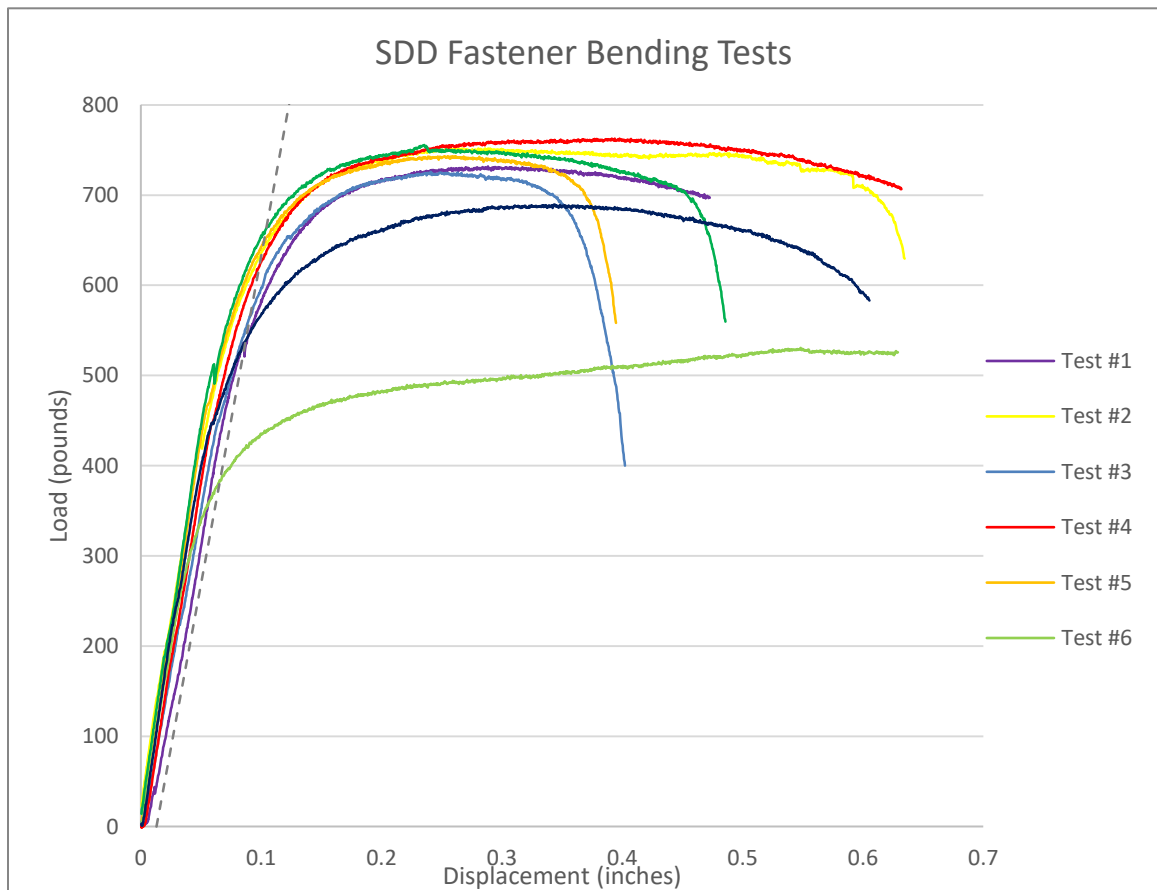


Figure 32 SDD bending test load-displacement

The bending failures initiated at the root of the thread directly under the center load point on the tension face of the fastener. The fasteners maintained a linear load deformation response for the initial portion of loading as shown in Figure 32 and then experience a significant amount of deformation while maintaining the ultimate load. Following the fracture on the tension face of the fastener, an abrupt loss of load took place except for in test six. In test six the fracture initiated prematurely at approximately 350 lbs and maintained load until the fastener reached the maximum allowable displacement for the test assembly. Failures of the eight bending test specimens are shown in Figure 33.



Figure 33 SDD bending failure

The fastener shear tests were performed to determine the allowable shear strength of the fasteners. The test method used a double shear test setup (Figure 16) rather than the single shear test setup specified in AISI TS-4-02 (American Iron and Steel Institute, 2001) to enable the setup to be reused for each test. The maximum load reached prior to shear failure was averaged for all seven tests and reduced by a factor of three to provide an allowable shear strength for the fasteners of 1725 lbs as published by MyTiCon. Results of the fastener shear strength tests are shown in Table 3 and the shear load-displacement response of the SDD fasteners is shown in Figure 34.

Table 3 SDD Shear Test Results

SDD Shear Test Results	
Test Number	Maximum Load (lbs)
Test #1	11016
Test #2	10547
Test #2	9796
Test #3	10500
Test #4	10086
Test #5	10357
Test #6	10205
Average	10358
COV	3.7%



Figure 34 SDD shear test load-displacement

The load-displacement response for test one obtained a steeper loading curve relative the other tests. The bottom steel bar supports in the test assembly experienced a slight material loss on the inside vertical faces as the fastener sheared and pushed downwards between bearing points. Due to the less defined shear planes the fasteners in tests three through seven experienced a bending response prior to transitioning into a shear response as seen in the steepening of the load curve at approximately 0.8 in. The bending response can be seen in some of the tested specimens shown below in Figure 35. The data acquisition was disrupted during the initial loading of test specimen two as seen

in Figure 34 where the early portion of the load curve is not present. The load-displacement response for tests three through seven provided very consistent results and the ultimate loads for all seven tests provided a low COV of 3.7 percent. When the ultimate load capacity was reached, a sudden shear failure occurred, resulting in a rapid loss of load.



Figure 35 SDD shear failure

Single Knife Plate Tests

Two setups were tested using single knife plates to determine the dowel bearing strength of each connection and verify the yield mode for single and group fastener configurations. The average coefficient of variation (COV) for various wood mechanical

properties published in the Forest Product Laboratory Wood Handbook (Forest Products Laboratory, 2010) are shown in Figure 36. The COV estimates for the mechanical properties of wood in compression are 18 to 24 percent depending on orientation of the wood grain while the typical COV for dowel bearing tests specified in ASTM D 5764 – 97a (ASTM International, 2002) range from 15 to 30 percent. The results of the testing provided consistent load deformation responses within acceptable COV limits for dowel bearing tests as shown in Table 4.

Property	Coefficient of variation ^a (%)
Static bending	
Modulus of rupture	16
Modulus of elasticity	22
Work to maximum load	34
Impact bending	25
Compression parallel to grain	18
Compression perpendicular to grain	28
Shear parallel to grain, maximum shearing strength	14
Tension parallel to grain	25
Side hardness	20
Toughness	34
Specific gravity	10

^aValues based on results of tests of green wood from approximately 50 species. Values for wood adjusted to 12% moisture content may be assumed to be approximately of the same magnitude.

Figure 36 Coefficients of variation for clear wood mechanical properties (Forest Products Laboratory, 2010)

The testing methods were based on ASTM D 5764 – 97a (ASTM International, 2002) but used the single knife plate setups shown in Figure 17 and Figure 18 rather than the half or full hole test setups prescribed in the standard. The variation in the test setup allow for validation of the yield mode fastener bearing calculation set forth in the NDS. A

summary of the single knife plate single and group fastener test results can be found in Table 4 and Table 5 and the load-displacement response of the single and group fastener configurations are shown in Figure 37 and Figure 38.

Table 4 Single Knife Plate Single Fastener Test Results

Single Knife Plate Single Fastener Results	
Test Number	Maximum Load (lbs)
Test #1	3746
Test #2	3254
Test #3	3712
Test #4	3730
Test #5	2886
Test #6	4077
Average	3567
COV	11.9%

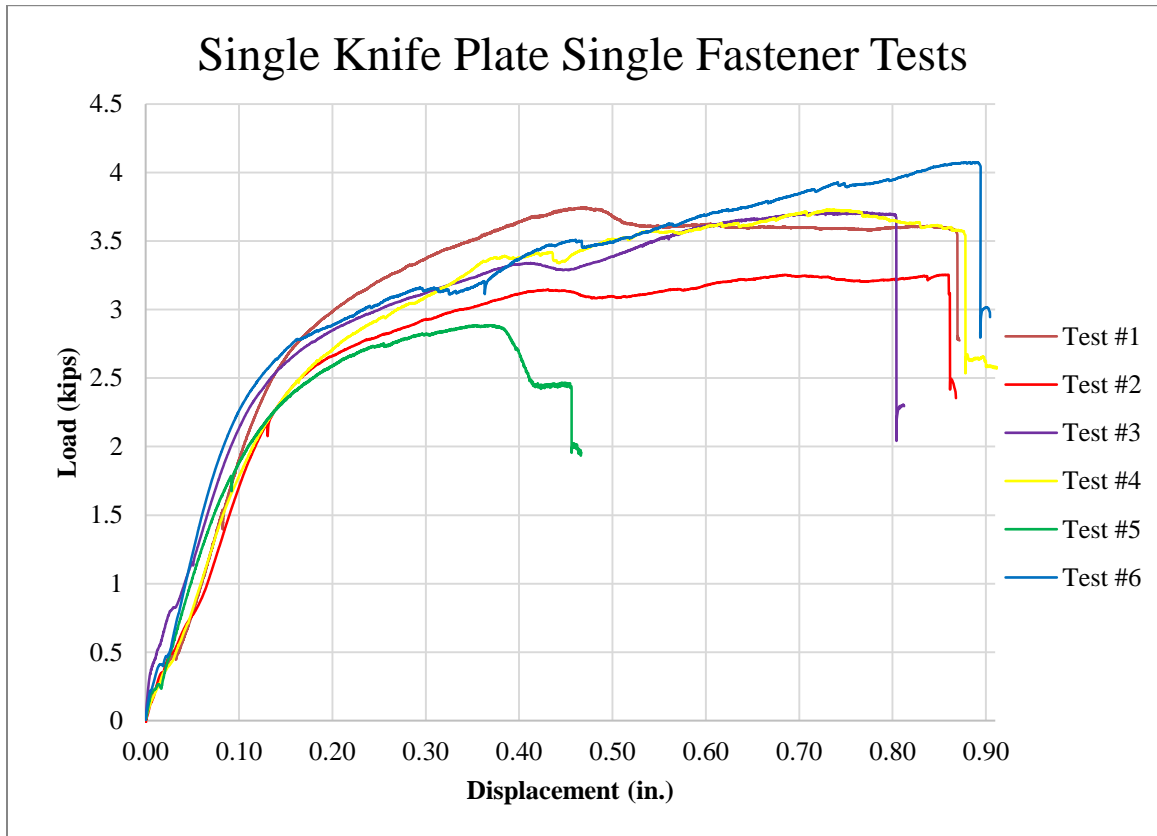


Figure 37 Single knife plate single fastener load-displacement

Table 5 Single Knife Plate Group Fastener Test Results

Single Knife Plate Group Fastener Results	
Test Number	Maximum Load (lbs)
Test #1	18282
Test #2	18821
Test #3	22748
Test #4	18977
Test #5	18209
Test #6	17096
Average	19022
COV	10.2%

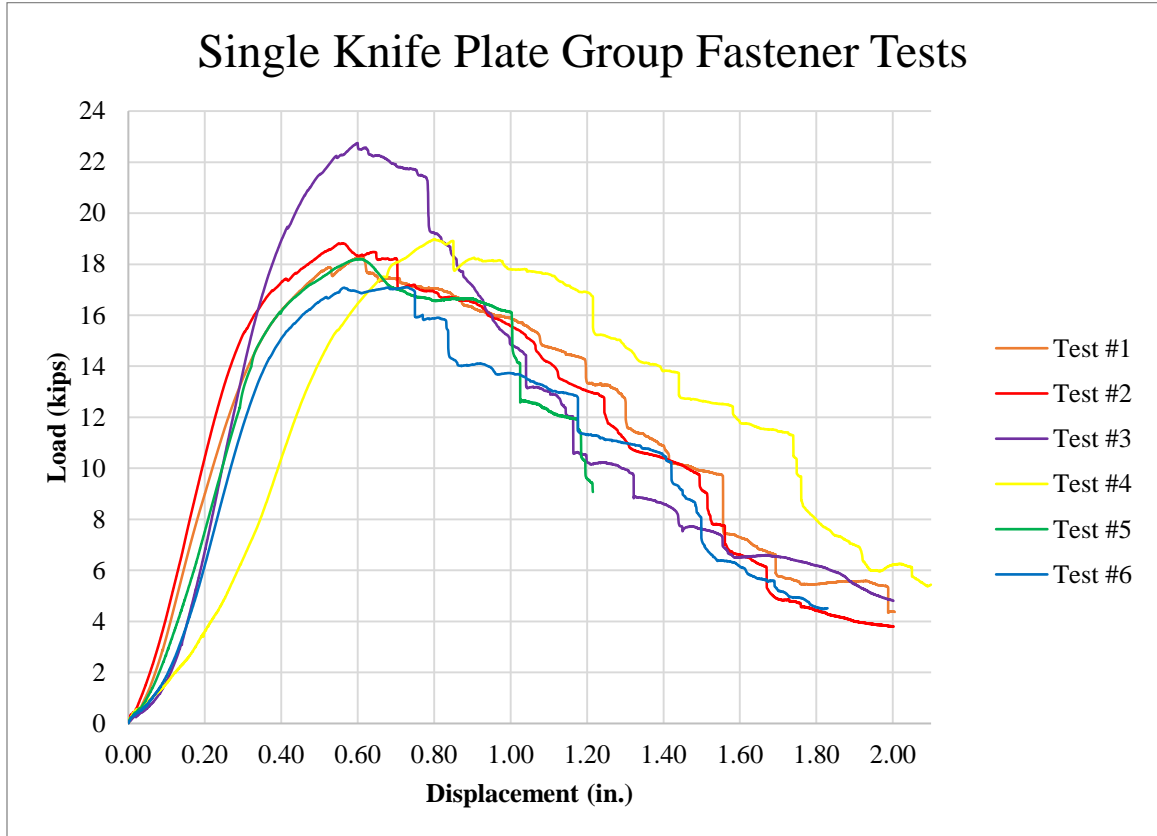


Figure 38 Single knife plate group fastener load-displacement

The yield mode for both the single and group fastener tests using a single knife plate consistently displayed as mode III_s per Figure 30 as shown in Figure 39 and Figure 40. The single fastener failure shown in Figure 39 was for the last fastener tested in the CLT specimen and was pulled completely out of the panel using the MTS test frame. Half of fastener sheared off and resulted in a sudden loss of load as indicated in Figure 37. The values for the group fastener tests compared very closely to individual fastener tests but did display a small group action response. The group action factor from the NDS accounts for the bulk section of the main and side members which must be assumed for a

CLT panel, but when using an assumed 5.5 in. wide portion of the panel should have been negligible for the connection geometry.

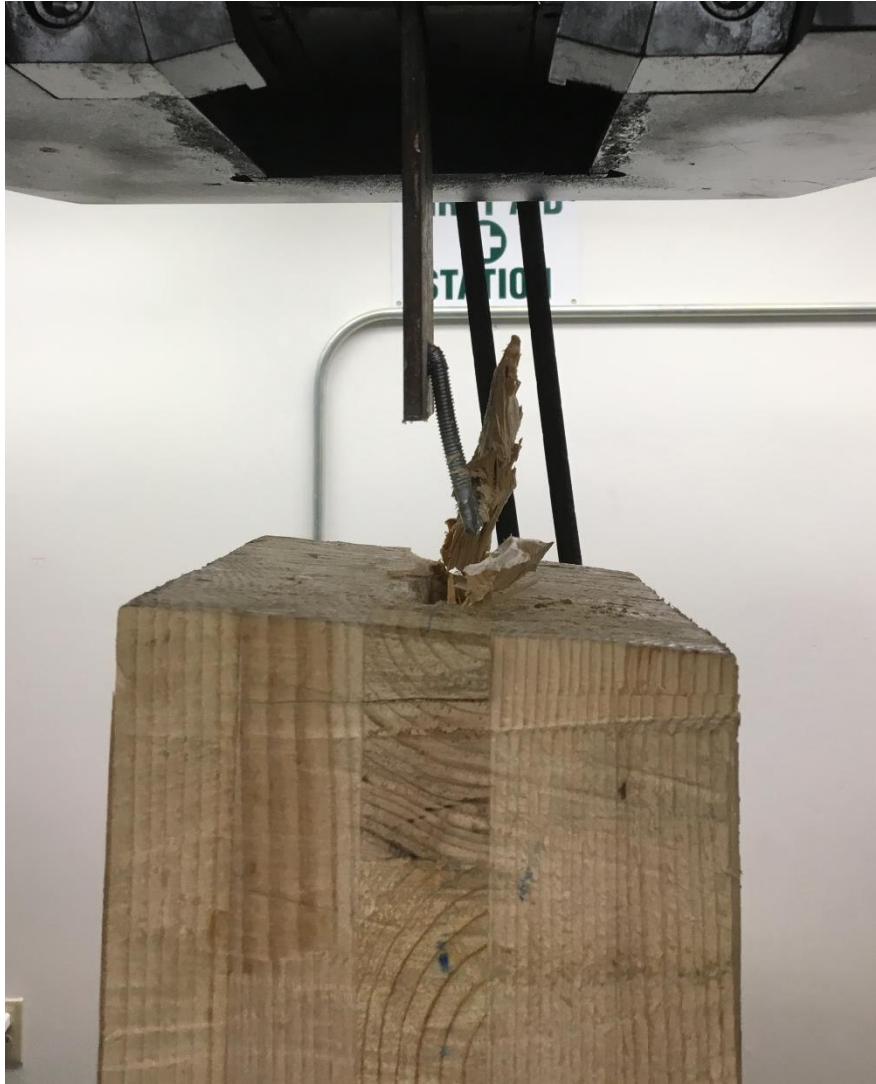


Figure 39 Single knife plate single fastener failure



Figure 40 Single knife plate group fastener failure

The load-displacement response allowed for a substantial amount of deformation in the CLT panel and fastener prior to reaching the ultimate load. A small amount of connection slip can be seen at the beginning of the load-displacement response for the group fastener tests due to seating of the bolted connection layout. The lack of initial connection slip displayed in the single fastener tests is due to the connection at each end of the CLT specimen utilizing the SDD fasteners rather than a bolted connection. The SDD fasteners drill through the remaining wood and steel material when driven into the panel alleviating the need to oversize the pilot holes to allow for bolts to be placed. This provides a good representation of the tight-fitting connections that can be developed

using SDD fasteners compared to bolted connections. Any slip in the fastener connection for the holdown assembly in this project results in larger lateral deflection at the top of the CLT panel and limits the energy dissipation that can be achieved through yielding of the steel plate while maintain allowable drift constraints. The comparison between the single and group fastener load-displacement responses confirms that the SDD fasteners are an excellent choice for the intended holdown application.

Double Knife Plate Tests

Following results of the single knife plate tests, the connection configuration was modified to a double knife plate to optimize the use of each fastener. The double knife plate connection develops a slightly stiffer response in the linear loading phase and reduces the number of fasteners required to develop the desired capacity. The double knife plate tests followed the same testing method used to complete the single knife plate tests for a direct comparison between the two connection configurations. A summary of the double knife plate single- and group-fastener test results can be found in Table 6 and Table 7 and the load-displacement responses of each configuration are shown in Figure 41 and Figure 42. The COV for both fastener configurations were very low for wood connections (8.7% and 6.5% for the maximum load) and provided more consistent results than the single knife plate tests (Table 4 and Table 5).

Table 6 Double Knife Plate Single Fastener Test Results

Double Knife Plate Single Fastener Results	
Test Number	Maximum Load (lbs)
Test #1	5035
Test #2	6325
Test #3	5235
Test #4	5086
Test #5	5547
Test #6	5500
Average	5455
COV	8.7%

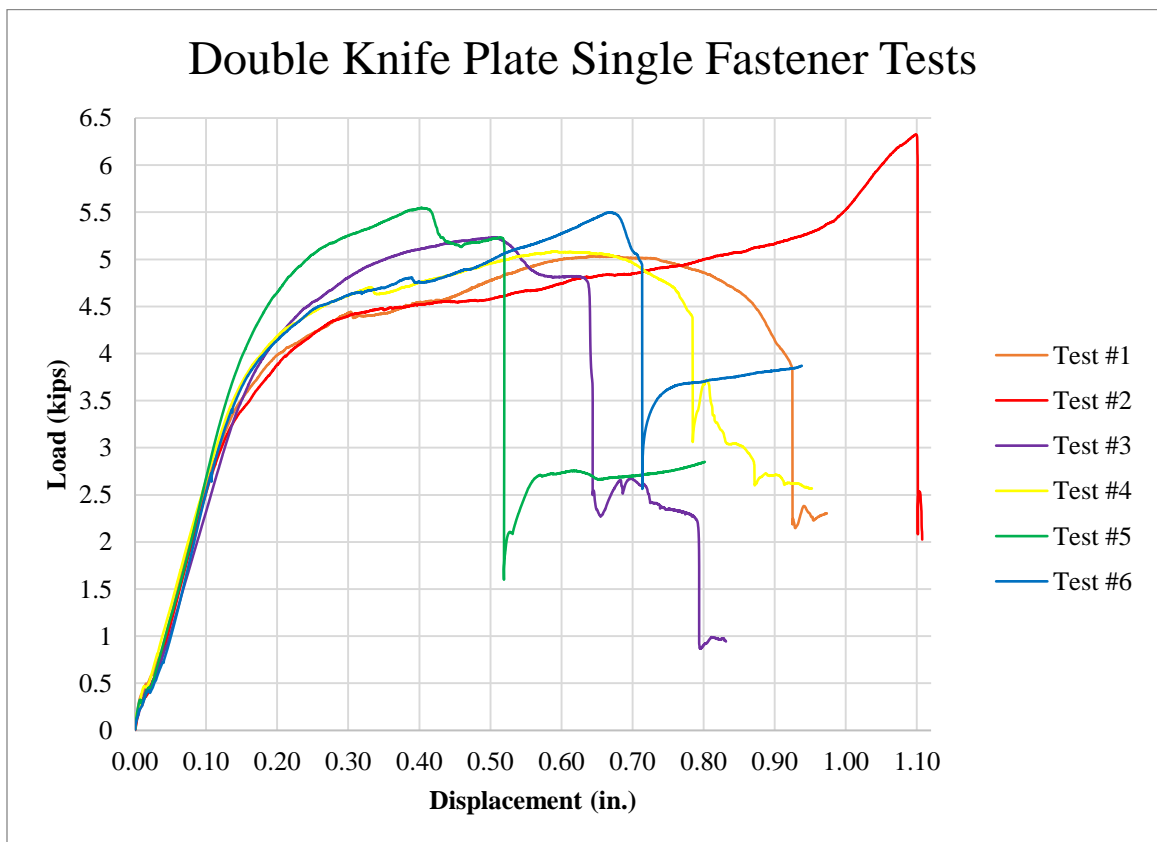


Figure 41 Double knife plate single fastener load-displacement

Table 7 Double Knife Plate Group Fastener Test Results

Double Knife Plate Group Fastener Results	
Test Number	Maximum Load (lbs)
Test #1	24059
Test #2	27175
Test #3	23410
Test #4	27073
Test #5	24719
Test #6	24085
Average	25087
COV	6.5%

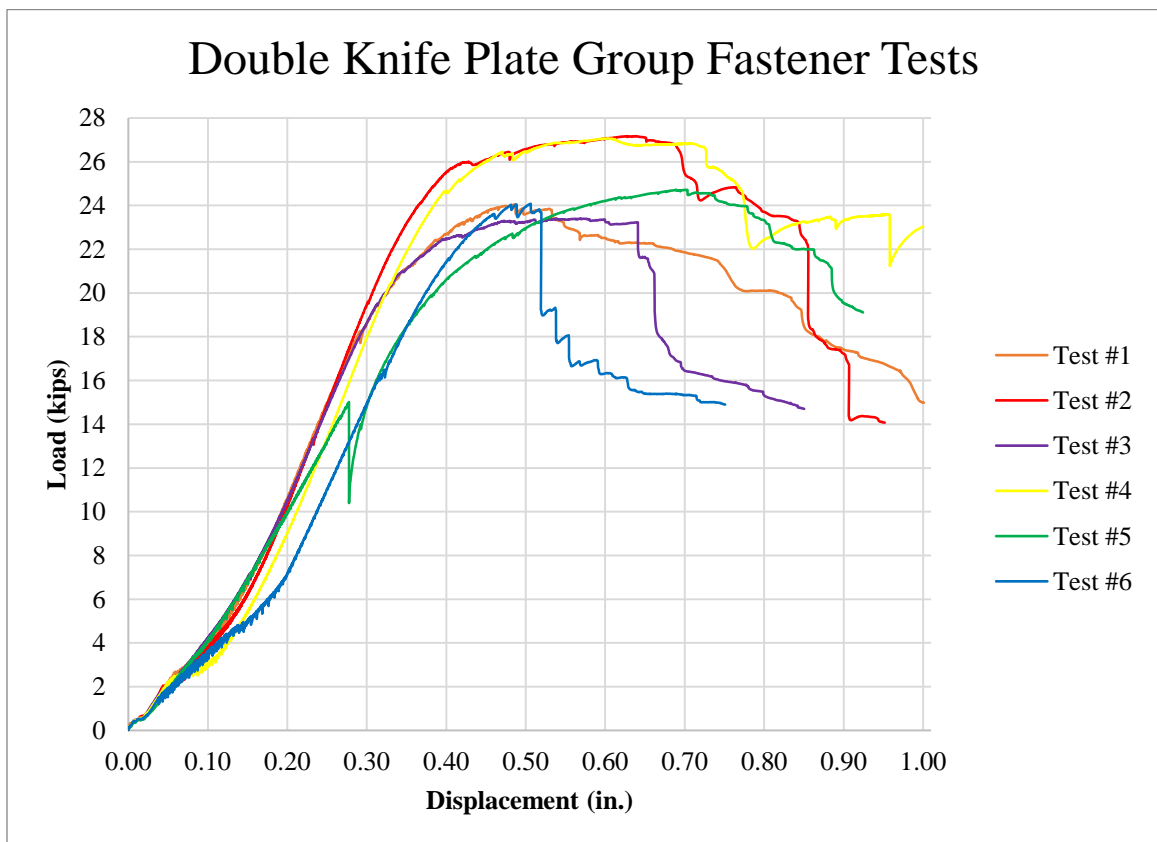


Figure 42 Double knife plate group fastener load-displacement

The double knife plate tests provided a 47 percent increase in the yield capacity of the fastener connection compared to the single knife plate configuration. The average deflection at the yield load for both configurations was very similar but the early load response was stiffer for the double knife plate configuration as shown in Figure 43. The results of the double knife plate testing verified that this configuration would be better for the holdown connection than the single knife plate configuration. It would reduce the number fasteners required by approximately one third and would provide a stiffer response in the load range desired for the fasteners. A direct comparison between the single and double knife plate group configurations can be seen in Figure 43 below.

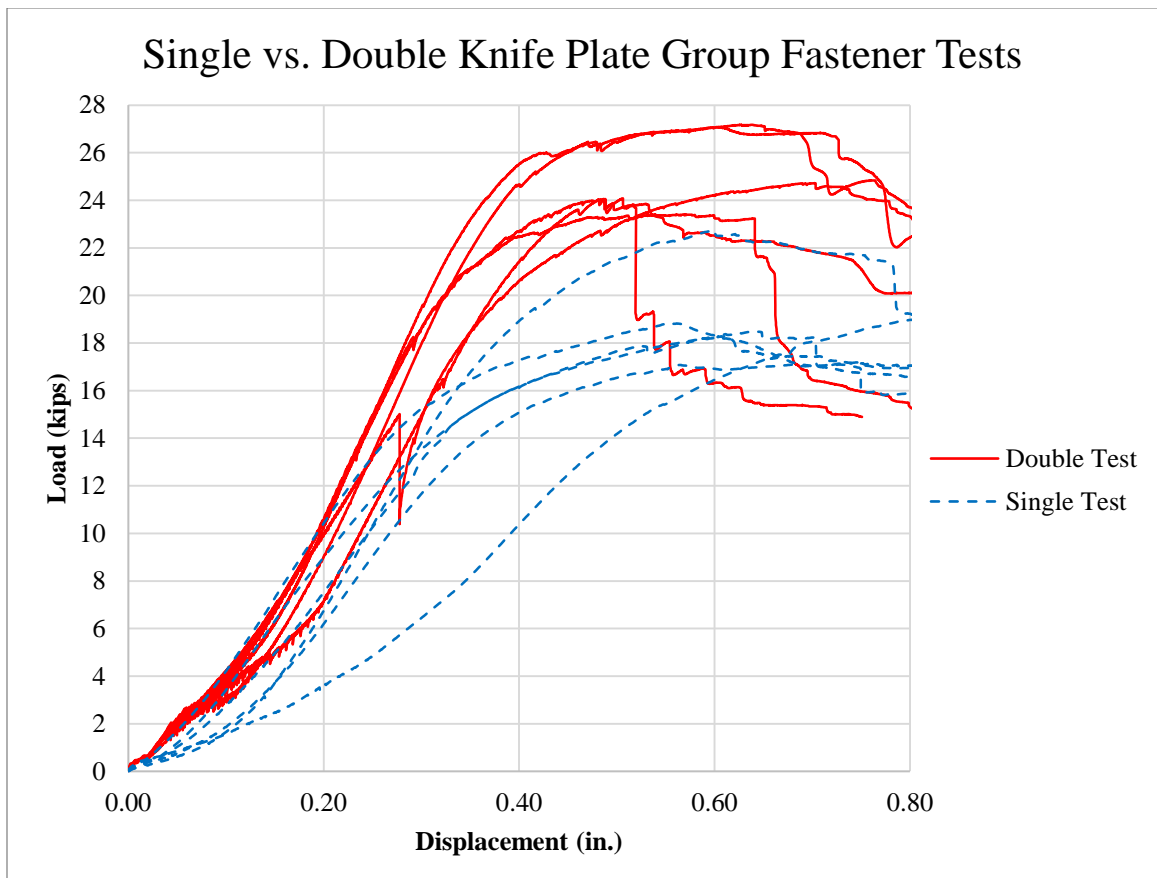


Figure 43 Single vs. double knife plate group fastener tests

Reduced Section Steel Plate Models and Tests

Prior to performing testing with reduced section knife plates, FEA modeling was completed using ANSYS to determine the optimal configuration for the reduced portion of the steel plate. Initial models used circular patterns similar to the perforated adhesive plates in the research performed by Zhang et al. (2018) for the reduced section in attempt to produce a plate design that could be easily manufactured by punching the steel plate rather than cutting it on a CNC machine. The circular pattern models formed vertical yield lines running between each row of holes limiting the volume of steel in yielding. By using diamond cutouts rather than circular cutouts yield lines were able to be formed diagonally across each remaining section of plate between to the cutouts similar to a strut and tie model. This pattern provides a larger volume of steel in yield and was determined to be a more efficient pattern for energy dissipation. The results of the initial models led to using elongated diamond cut outs as shown in Figure 25 to obtain a more uniform stress distribution over a larger volume of steel. The FEA models only included the yield zone of the reduced section pattern where yielding was expected.

Once the desired pattern for the relieved portion of the plates was determined, a small-scale model was created in ANSYS using the same geometry to be validated with a specimen that would fit in the MTS test frame. The geometry of the model extended to the exterior face of the stiffener plates where the weld from the stiffener plate to the reduced section plate was located as shown in Figure 23. The degree of freedom constraints used in the ANSYS model were more representative for the full-scale holdown assembly than the small-scale tests due to the rotation that occurred at each side

of the small-scale test specimen. The results of the small-scale testing, however, aligned reasonably well with the model. The deflected shape plot from the ANSYS model can be seen in Figure 44 and the Von Mises element stress plot can be seen in Figure 45. The vertical nodal displacement used along the right edge of the plate for the displacement and stress plots shown was 0.3 in.

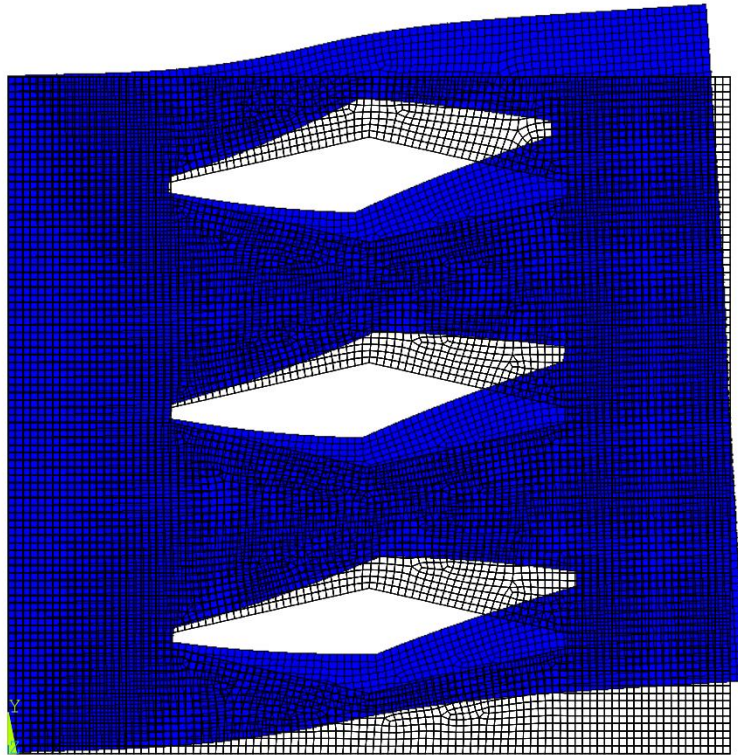


Figure 44 ANSYS small-scale plate element deflection plot

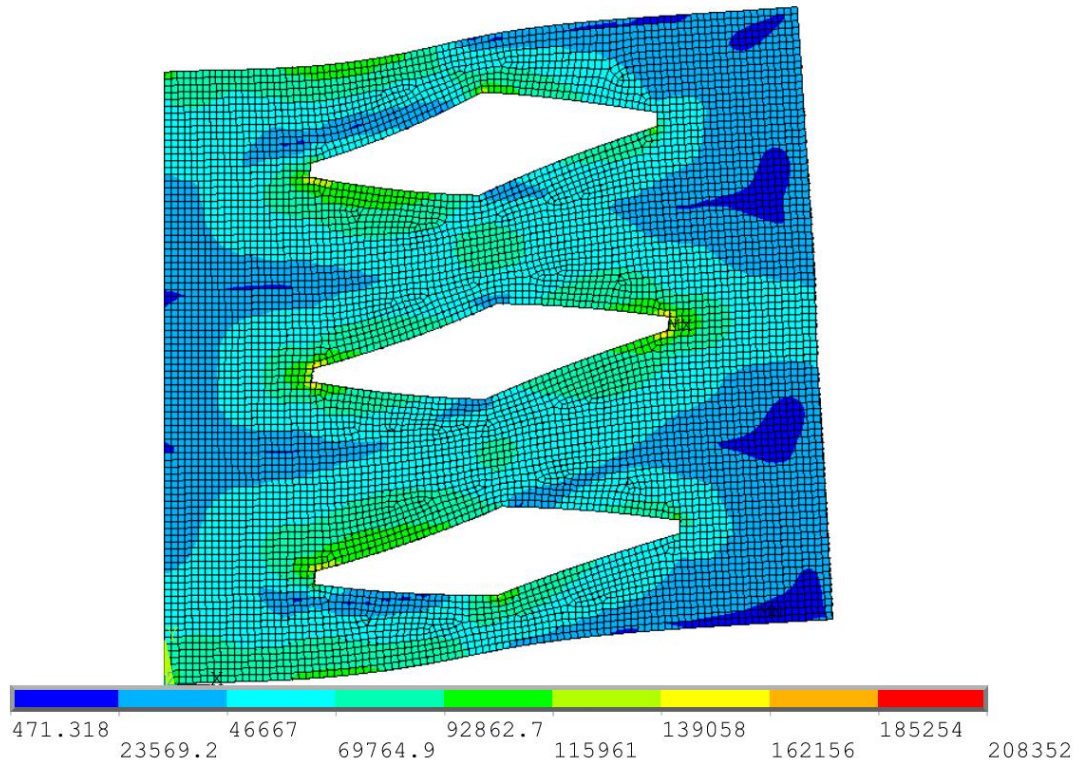


Figure 45 ANSYS small-scale Von Mises element stress plot

As seen in the element stress plot for the small-scale model, the relieved pattern (Figure 23) achieves yield stresses throughout a substantial amount of the desired yield zone. The element stresses shown in Figure 45 are in units of pounds per square inch. Stress concentrations develop at the edges of the relieved portion of the plate that could have been addressed by filleting the corners with a radius. If subjected to many cycles it is likely that fatigue cracks could develop at these locations. However, the testing performed in this research was not adequate to determine the behavior of the plate under these conditions. For the purpose of simplifying the plate geometry in the FEA model and creating a mesh that would perform well using quadrilateral elements the radii were not incorporated into the model or the final reduced section layout. The plots of element

stresses shown for the small-scale plate were approaching the maximum number of elements allowed when using the ANSYS license available at Montana State University and did not allow for refining the mesh beyond this point without increasing the element size toward the sides of the plate model. Based on the element stress plot convergence it was determined that the number of elements used was sufficient for the general plate behavior, but additional refinement may have been necessary to study the stress concentrations that were forming at the corners of the reduced sections.

Once the FEA modeling was completed for the small-scale plates, the resulting geometry was cut on a CNC laser machine to be tested in the MTS test frame. The maximum width of the plate assembly that would fit in the MTS test frame was 5 in. which controlled the size of the small-scale plates. Vertical tabs were left on each side of the plate to allow for the specimen to be subjected to a tension load test. The displaced shape of the tested specimen shown in Figure 46 aligns well with the FEA model. The rotation at the sides of the plate were balanced between each edge rather than forced to one side as previously discussed.

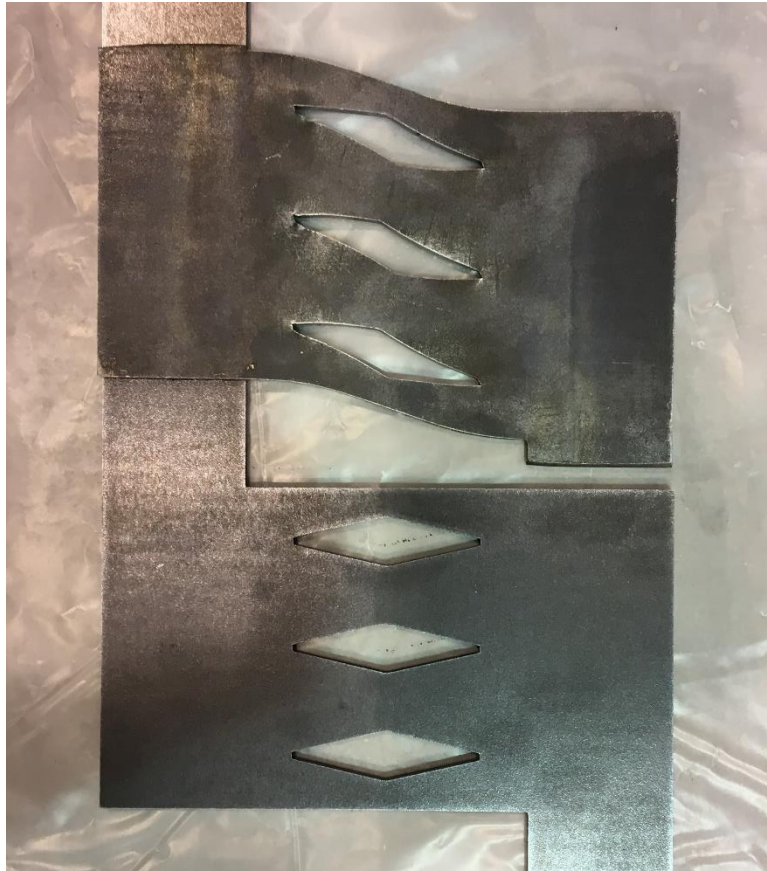


Figure 46 Small-scale reduced section deformed plate

The load-displacement response of the FEA model was slightly stiffer than the response of the specimens tested in the MTS as shown in Table 8 below. Due to the slender width of the loading tabs used for the assembly to fit in the MTS test frame and the eccentric load created by the test setup, the loading tabs yielded at the top of the stiffener plates throughout the test as shown in Figure 47 contributing to the load-displacement response. The total vertical displacement in the yield zone shown in Figure 46 for test 1 was approximately 0.625 in. and for test 2 was approximately 0.75 in. The bending deformation in the loading tabs contributed to the displacement throughout the test due to the tabs bending as shown in Figure 47. Most of the tab bending deflection

contribution occurred beyond 0.35 in. but a small amount was seen in the early loading stage. The increased stiffness response of the analytical model was likely due to the boundary conditions assigned to the model, the loading tab bending deflection and the small amount of deflections that occur in the MTS test frame during initial loading. The load-displacement curve for the specimens tested in the MTS test frame are shown in Figure 48 below.

Table 8 Small Scale Plate Reaction Summary

Displacement (in.)	ANSYS Reaction (lbs)	MTS Test #1 (lbs)	MTS Test #2 (lbs)
0.2	3535	3070	3222
0.3	4246	3993	4102



Figure 47 Small scale loading tab displacement

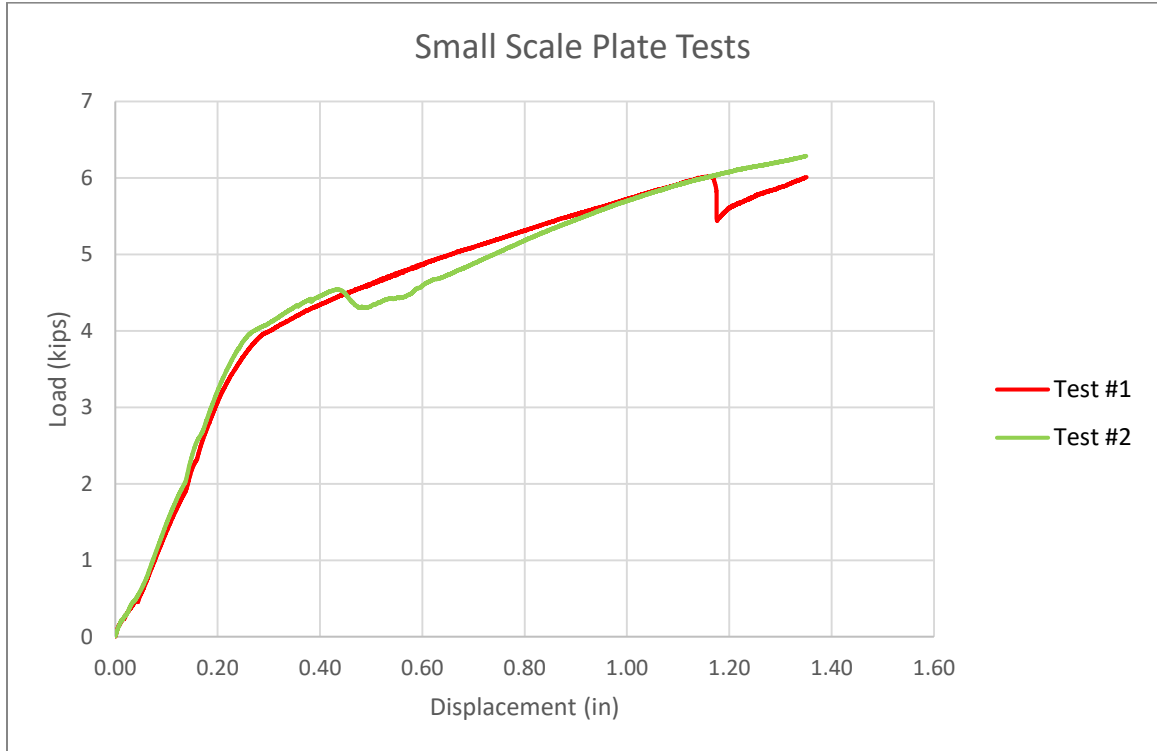


Figure 48 Small-scale reduced section load-displacement curve

CLT Shear Wall Test

Once the FEA model for the reduced section steel plates had been validated, the design was scaled to accommodate the target load of 75 kips at a displacement of 0.3 in. The scaled model used 18 identical diamond shaped cutouts evenly spaced along the length of the steel plate to provide a uniform load and stress distribution along the plate. The resulting FEA model displaced shape can be seen in Figure 49 and the Von Mises elements stress plot can be seen in Figure 50. Only the upper portion of the plate is shown in these figures to highlight the displaced shape and stresses, but the model contained the

total geometry of the yield zone shown in Figure 25 extending 0.5 in. on each side of the relieved portions of the plate. Similar stress concentrations at the edges of the cutouts can be seen in the full-scale model that could be addressed using radii at the effected corners. The stress concentrations along the right edge of the plate would be resolved due to the increased width of the plate to allow for the fasteners.

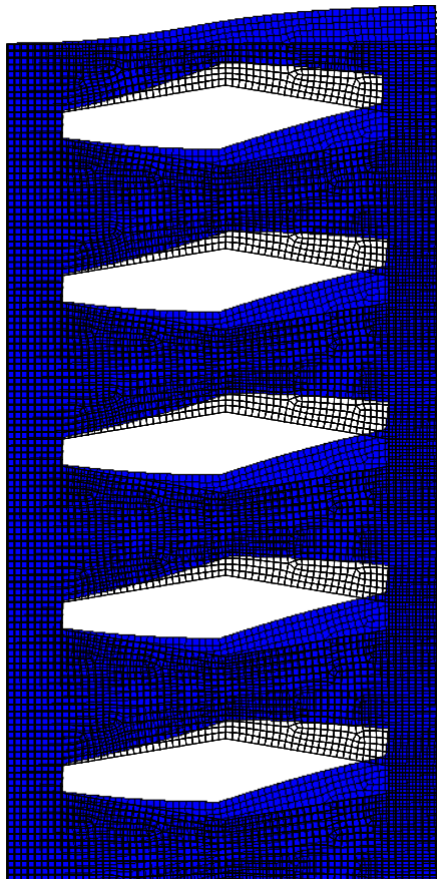


Figure 49 ANSYS full-scale plate element deflection plot

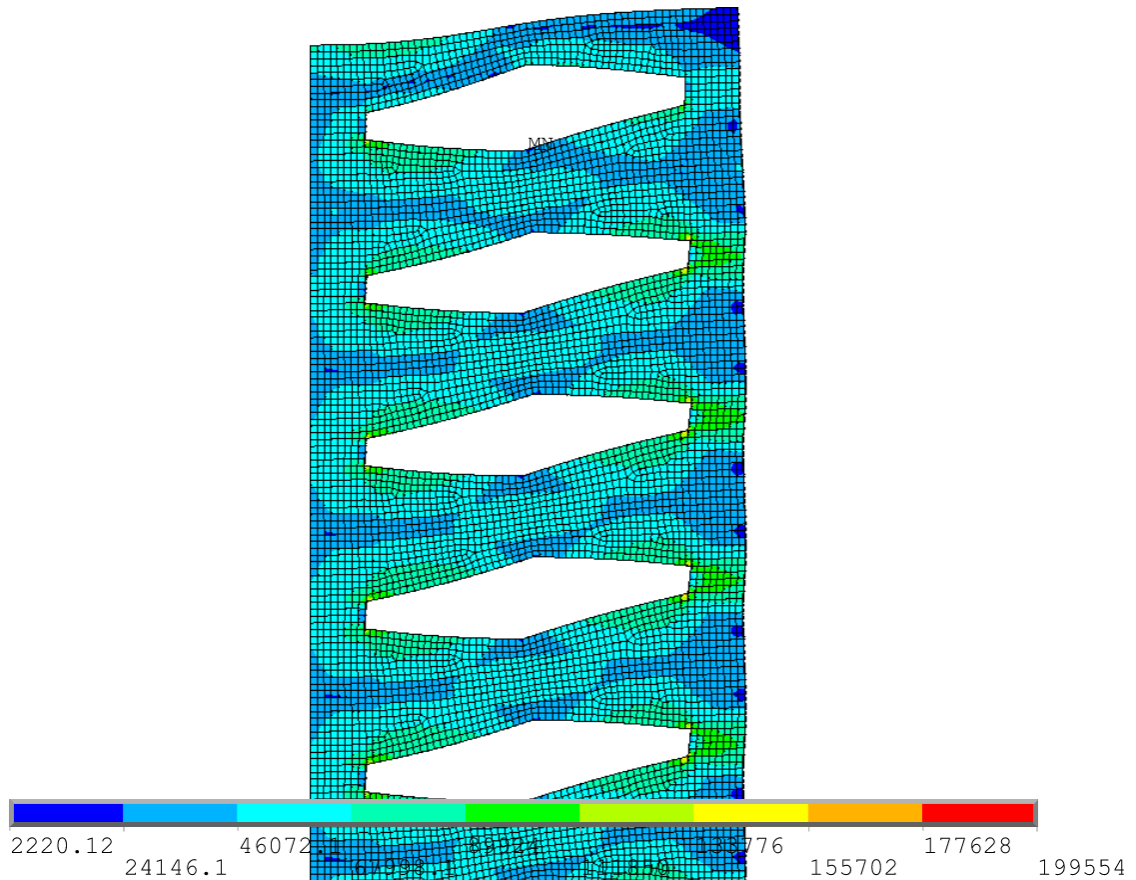


Figure 50 ANSYS full-scale plate Von Mises element stress plot

The intended CLT panel height for the shear wall system was 10 ft, however, the final test setup implemented a 5.9 ft. tall panel (Figure 26). The shorter CLT panel increased the lateral load required to obtain the targeted uplift force beyond the capacity of the loading setup. In the initial setup for testing the pressure transducer was not functioning correctly and required the addition of an external load cell to the loading assembly. The addition of the load cell increased the eccentricity and resulted in an unstable configuration. The lack of bracing to prohibit out-of-plane panel movement and the eccentric loading from the addition of the load cell led to the panel rising off the ground at higher applied loads. The required load to yield the holdown assembly was not

able to be reached using the test assembly that was constructed, prohibiting the development of clearly defined hysteresis loops, however, the following data can provide a foundation for future research to be completed.

The shear wall tests began with a half cycle by applying load to the upper right corner of the CLT panel (Figure 26). The targeted CLT panel vertical displacement at the lower corner for the first cycle of loading was 0.1 in. The shear wall assembly achieved the vertical panel displacement at a lateral applied load of 23.1 kips and a holdown force of 45.1 kips. The approximate lateral load-displacement response measured at 5 ft from the base of the panel can be seen in Figure 51 and the vertical CLT panel load-displacement plot for all completed cycles can be seen in Figure 52. As shown in the lateral load-displacement response the shear wall assembly exhibited much less rigid behavior than expected under the applied lateral load. However, substantial contributions to the lateral displacement were a result of the test setup. The calculated lateral displacement due to CLT panel deflections for the specimen in the initial cycle at 5 ft from the base of the panel was approximately 0.054 in., if considering all plies for the moment of inertia. After loading the specimen to a lateral displacement of 1.37 in., the rebound was 0.8 in, compared with a rebound of only 0.04 in. for the vertical displacement measurements (Figure 51). The difference in these deflection measurements suggest a large amount of lateral panel deflection was a result of the test setup rather than the shear wall assembly.

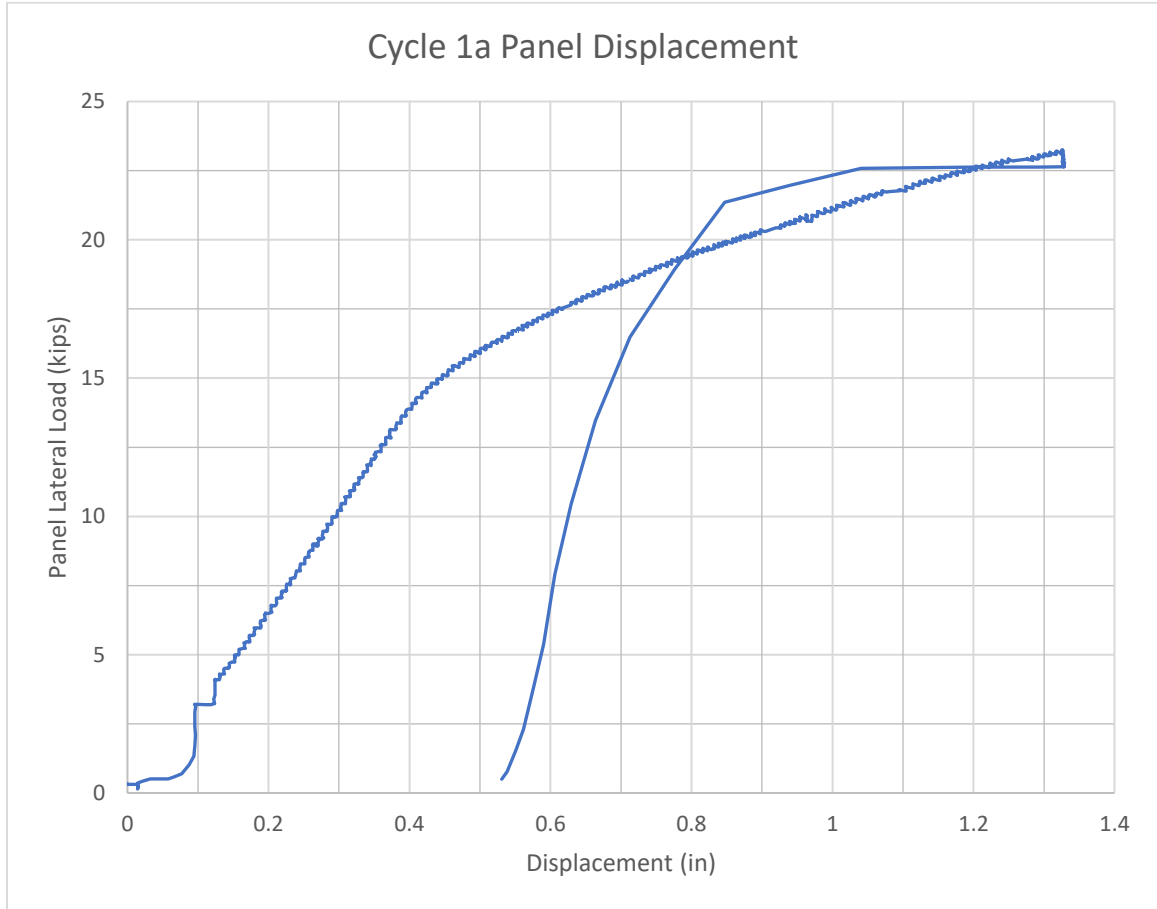


Figure 51 CLT shear wall cycle 1a lateral load-displacement plot

There are many sources within the test setup that contributed to the lateral displacement shown in Figure 51. The 1.25 in. diameter Dwyidag bar post-tensioned to the strong floor through a 2 in. diameter hole relied on friction between the HSS anchorage member and the concrete slab to prevent the lower corner of the panel from moving. The friction force between the HSS and the concrete was not sufficient to provide a rigid anchor point for the lower right corner of the CLT panel. Much of the lateral displacement was contributed by movement at the anchorage point, which is amplified by a factor of approximately 1.8 when relating the anchorage displacement

aligning with the uplift force to the lateral panel displacement at the location of the displacement measurement. In the worst-case scenario, the lateral displacement could have been skewed by 1.33 in. of deflection due to the sliding HSS. This was seen in the lateral load-displacement plots for all cycles following the first half cycle. The vertical panel displacements were measured from the HSS at the base of the panel (Figure 26), rather than the concrete floor to provide relative displacements and are a more accurate representation of the system behavior.

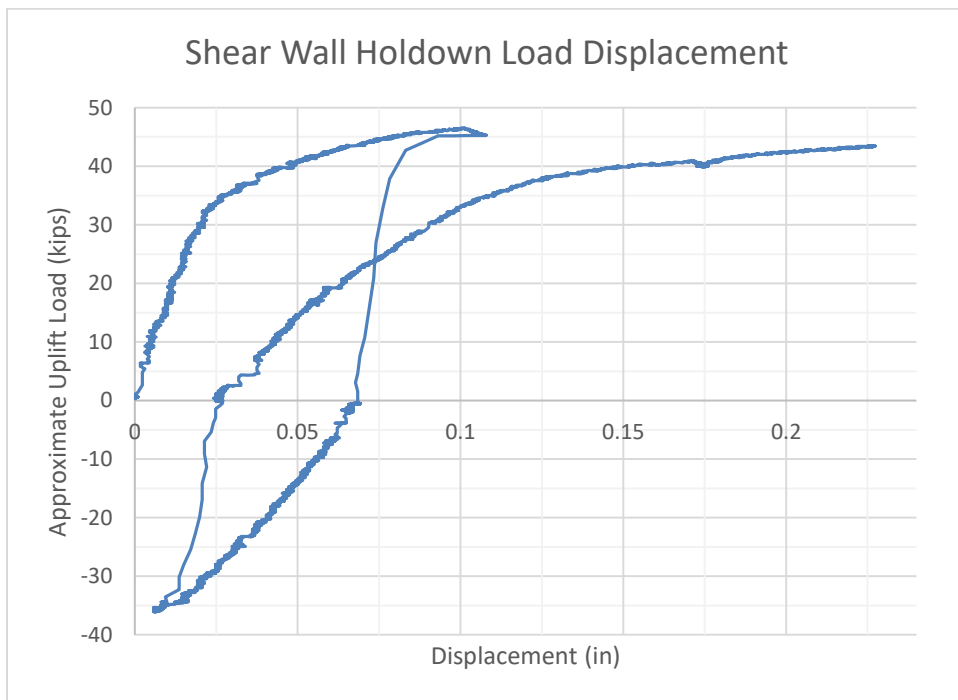


Figure 52 CLT holddown vertical load-displacement plot

The vertical displacements measured during 1.5 load cycles show the beginning of a robust hysterical response desired for seismic loading, however, the holddown forces did not provide enough load to cause yielding in the desired location of the reduced section steel plates as shown in Figure 53. To determine the true system response the test

setup needed a larger capacity, or the plates needed to be adjusted to yield at a lower load. The fasteners did not show significant signs of yielding, as shown in Figure 54 and the CLT panel experience very little wood crushing as shown in Figure 55 indicating that a significant portion of vertical load-displacement response may have been a result of the test setup rather than the shear wall assembly. The exposed faces of the panel showing the fastener holes in Figure 55 were in contact with the knife plate closest to the fastener heads in the holdown assembly.



Figure 53 Tested full-scale reduced section knife plate



Figure 54 Tested shear wall fastener



3

Figure 55 Tested CLT panel fastener holes

Due to the lack of out-of-plane bracing and eccentric loading, the panel was eventually thrust away from the concrete floor during the second load cycle forcing the welds to the HSS anchorage member to resist bending forces in addition to the uplift force. The combination of the moment induced on the wall of the HSS member and the post-tension force applied to the top of the anchorage member forced the HSS wall in contact with the bottom of the CLT panel to buckle. The buckling deformation in the wall of the HSS caused the welds to crack as shown in Figure 56. Following this event, it was determined that it would be not be safe to continue testing the specimen using the inadequate testing assembly.



Figure 56 HSS wall buckling failure

Although the shear wall test was not able to measure the yield strength of the shear wall assembly or holdown behavior, it did provide insight into design

considerations for this holdown connection configuration. The shear wall panel, fastener connection and the anchorage would need to be designed to provide a very stiff load-displacement response so that the primary source of displacement is limited to the holdown assembly. Slender panels require a more stringent vertical holdown deflection limitation to maintain allowable lateral drifts at the top of panel compared to panels with lower height to width aspect ratios. Due to the deflection sensitivity of holdowns on slender panels, the connection assembly utilized in this research would likely not be a good option for panels with high aspect ratios. A thicker plate that limits stretching during yielding may be a better option if applying the connection methods in this research to slender shear walls.

As you reduce the aspect ratio of the panel, the allowable vertical deflection for the holdown based on drift limitations increases, making the assembly used in the shear wall test more suitable for building drift limitations. Detailing of the surrounding building elements would need to be considered to accommodate the increased vertical deflections. However, the larger allowable vertical deflections would enable the system to take advantage of the energy dissipation that can be provided through large displacement yielding of the reduced section plate.

SUMMARY & CONCLUSION

The primary objective of this research was to provide insight into wood connections that utilize reduced-section steel plate connectors to perform as ductile elements rather than developing ductility from the fastener interaction with a wood element. The research completed in this thesis touches on many concepts that are useful for structural connection design in heavy and mass timber projects. Although the research performed utilized a holdown connection for CLT panels, the same energy dissipation mechanisms could be applied to various connections within mass timber structures.

The self-drilling dowel fasteners used for this project enable a convenient field installation process for many types of connections that create aesthetically pleasing high capacity connections. The fastener response to loading provides a ductile failure at ultimate capacities, which helps avoid brittle failures while maintaining enough stiffness to be used in deflection sensitive connections. The tight fit developed between a concealed steel plate and a wood member makes the fasteners ideal for deflection sensitive shear connections that utilize knife plates. The fastener testing in this research provides ultimate loads that can be used to validate design values for SDD fasteners in single and double knife plate assemblies. The high bending yield strength of the SDD fasteners provides a rigid response relative to traditional bolted connections of similar diameter and allows for concealed connections without the need to countersink the bolt heads. The SDD fasteners can be used to obtain high capacities and decrease field installation time.

The reduced-section plate modeling and testing provide insight into steel plate connections that can be used for shear transfer between wood elements to develop greater ductility in response to cyclic loading. When properly designed, reduced-section steel plates can enable greater ductility than traditional wood connectors for seismic force-resisting systems that cannot rely on a redundant number of fasteners to obtain energy dissipation. For wood lateral systems that are not inherently ductile, this connection style offers an alternative solution for achieving energy dissipation. The modeling completed in this project provides a foundation for future research to be completed on efficient patterns for reduced section steel plates.

The CLT shear wall test offers an example of design considerations when utilizing ductile plate connections, and steps that must be taken prior to performing testing to achieve meaningful output. The shear wall test reiterated the importance of considering the entire structural system behavior to ensure that the system can perform as intended.

In conclusion, the connection methods used in this research are suitable for providing ductility to lateral force-resisting systems that are not inherently ductile. The connection would perform well in shear wall systems assuming that the building was detailed to allow for enough deflection to enable successive yielding of the steel plate connector. The reduced section holdowns would perform best in combination with concealed-panel splice connectors that incorporate the same connection strategy, rather than solely a holdown that is intended to be the primary source of ductility. Utilizing the holdown in this research in a multi-panel wall with reduced section panel splice

connectors would allow for the panels to displace enough to yield a larger number of panel splice connectors, offering more energy dissipation and redundancy to the lateral force-resisting system.

FUTUTRE WORK

There is a large volume of future work that could be performed to expand on the research contained in this project. Moment resisting connections using SDD fasteners and concealed knife plates would be a suitable project to allow for concealed member splices and other forms of moment resisting connections in wood structures. Additional research on the behavior of reduced section steel plate connectors needs to be completed for this connection style to be implemented into practice. The overall system behavior of mass timber shear walls utilizing reduced section steel plate connectors could be completed to determine the feasibility of using this connection method in a structure. Incorporating the connection methods contained in this thesis in a combination of holdowns and panel splices to develop a system of ductile connections that offer redundancy and a high potential for energy dissipation would be a substantial research endeavor that could produce a well thought-out seismic force-resisting lateral system.

REFERENCES CITED

- American Iron and Steel Institute. (2001). *Standard Testing Method for Determining the Tensile and Shear Strength of Screws*. Retrieved from
- American Plywood Association. (2018a). *SmartLam Cross-Laminated Timber* (PR-L319). Retrieved from https://www.apawood.org/download_pdf.ashx?pubid=58c08d9e-9a78-4717-9bdd-e6807c070e84&bp=1
- American Plywood Association. (2018b). *Standard for Performance-Rated Cross-Laminated Timber* (ANSI/APA PRG 320-2018). Retrieved from
- American Society of Civil Engineers. (2010). *Minimum Design Loads for Buildings and Other Structures*. Retrieved from
- American Wood Council. (2017). *National Design Specification for Wood Construction 2018 Edition*. Retrieved from <https://www.awc.org/pdf/codes-standards/publications/nds/AWC-NDS2018-ViewOnly-171117.pdf>
- ASTM International. (2002). *Standard Test Method for Evaluating Dowel-Bearing Strength of Wood and Wood-Based Products* (D 5764 - 97a (Reapproved 2002)). Retrieved from
- ASTM International. (2008). *Standard Test Method for Determining Bending Yield Moment of Nails* (F1575 - 03 (Reapproved 2008)). Retrieved from
- AZoM. (2012, July 5, 2012). AISI 1018 Mild/Low Carbon Steel. Retrieved from <https://www.azom.com/article.aspx?ArticleID=6115>
- Forest Products Laboratory. (2010). *Wood Handbook - Wood as an Engineering Material* (FPL-GTR-190). Retrieved from
- Hossain, A., Danzig, I., & Tannert, T. (2016). Cross-Laminated Timber Shear Connections with Double-Angled Self-Tapping Screw Assemblies. *Journal of Structural Engineering*, 142(11). doi:10.1061/(ASCE)ST.1943-541X.0001572
- International Code Council. (2012). *International Building Code*. Falls Church, VA: International Code Council.
- Latour, M., & Rizzano, G. (2017). Seismic behavior of cross-laminated timber panel buildings equipped with traditional and innovative connectors. *Archives of Civil and Mechanical Engineering*, 17(2), 382-399. doi:10.1016/j.acme.2016.11.008

MyTiCon Timber Connectors. (2019). *Self-Drilling Dowel Design Guide*. Retrieved from <http://www.my-ti-con.com/resources/American-Self-Drilling-Dowel-Design-Guide>

Popovski, M., Schneider, J., & Schweinsteiger, M. (2010). *Lateral load resistance of cross-laminated wood panels*.

Think Wood. (2015). *Designing For Earthquakes*. Retrieved from <https://www.thinkwood.com/our-ceus/designing-for-earthquakes>

Zhang, X., Popovski, M., & Tannert, T. (2018). High-capacity hold-down for mass-timber buildings. *Construction and Building Materials*, 164, 688-703. doi:10.1016/j.conbuildmat.2018.01.019